

1 **Distinct mechanisms control the specific synaptic functions of Neuroligin 1 and**
2 **Neuroligin 2**

3 Jinzhao Wang^{1,2,4,5}, Thomas C. Südhof^{1,2,3,*} and Marius Wernig^{1,4,5,*}

4 ¹Institute for Stem Cell Biology and Regenerative Medicine

5 ²Department of Molecular and Cellular Physiology

6 ³Howard Hughes Medical Institute

7 ⁴Department of Pathology

8 ⁵Department of Chemical and Systems Biology

9 Stanford University School of Medicine

10 Stanford, CA 94305, USA

11 * co-corresponding authors

12 Emails: tcs1@stanford.edu; wernig@stanford.edu

13 **Key Words:** neuroligin, synapse specific, extracellular domain, intracellular domain,
14 distinct mechanisms

15

1 **Abstract**

2 Neuroligins are postsynaptic cell-adhesion molecules that regulate synaptic function
3 with a remarkable isoform specificity. Although Nlgn1 and Nlgn2 are highly homologous
4 and biochemically interact with the same extra- and intracellular proteins, Nlgn1
5 selectively functions in excitatory synapses whereas Nlgn2 functions in inhibitory
6 synapses. How this excitatory/ inhibitory (E/I) specificity arises is unknown. Using a
7 comprehensive structure-function analysis, we here expressed wild-type and mutant
8 neuroligins in functional rescue experiments in cultured hippocampal neurons lacking all
9 endogenous neuroligins. Electrophysiology confirmed that Nlgn1 and Nlgn2 selectively
10 restored excitatory and inhibitory synaptic transmission, respectively, in neuroligin-
11 deficient neurons, aligned with their synaptic localizations. Chimeric Nlgn1-Nlgn2
12 constructs reveal that the extracellular neuroligin domains confer synapse specificity,
13 whereas their intracellular sequences *are* exchangeable. However, the cytoplasmic
14 sequences of Nlgn2, including its Gephyrin-binding motif that is identically present in the
15 Nlgn1, *is* essential for its synaptic function whereas they *are* dispensable for Nlgn1.
16 These results demonstrate that although the excitatory vs. inhibitory synapse specificity
17 of Nlgn1 and Nlgn2 are both determined by their extracellular sequences, these
18 neuroligins enable normal synaptic connections via distinct intracellular mechanisms.

19

1 Introduction

2 Neuroligins (Nlgn) are evolutionarily conserved postsynaptic cell adhesion molecules
3 that bind to presynaptic neurexins (Nrns) (Ichtchenko *et al.*, 1995; Ichtchenko *et al.*,
4 1996; Nguyen & Sudhof, 1997). In vertebrates, four genes encode Nlgn: Nlgn1, Nlgn2,
5 Nlgn3, and Nlgn4. Among these, Nlgn1, Nlgn2, and Nlgn3 exhibit high conservation
6 across species, while Nlgn4 displays variability between rodents and humans and is
7 expressed at relatively low levels in mice (Bolliger *et al.*, 2008; Ichtchenko *et al.*, 1995;
8 Ichtchenko *et al.*, 1996; Jamain *et al.*, 2003). Nlgn are type 1 transmembrane proteins
9 that comprise a single, large extracellular domain consisting of a constitutively dimeric,
10 enzymatically inactive esterase-homology domain, a transmembrane region (TMR), and
11 a short cytoplasmic tail. Remarkably, the targeting of Nlgn to synapses is selective and
12 specific. Nlgn1 is only localized to glutamatergic synapses (Song *et al.*, 1999) while
13 Nlgn2 is exclusively present at GABAergic, dopaminergic, and cholinergic synapses
14 (Graf *et al.*, 2004; Takacs *et al.*, 2013; Uchigashima *et al.*, 2016; Varoqueaux *et al.*, 2004).
15 Nlgn3 is found in both excitatory and inhibitory synapses (Budreck & Scheiffele, 2007),
16 and Nlgn4 functions in glycinergic synapses in mice and in GABAergic synapses in
17 human neurons (Hoon *et al.*, 2011; Marro *et al.*, 2019; Zhang *et al.*, 2018). Consistent
18 with their localization to synapses, Nlgn perform multiple synapse-specific functions.
19 Compelling initial evidence supporting the synaptic function of Nlgn was obtained
20 through overexpression experiments, which demonstrated significant increases in
21 synapse density and synaptic transmission in transfected neurons (Chubykin *et al.*, 2007;
22 Scheiffele *et al.*, 2000). Since then, a large number of functional studies in invertebrates
23 and vertebrates using both deletions and mutations in Nlgn genes revealed a panoply
24 of important roles for Nlgn in shaping synapses, confirming the central contribution of
25 Nlgn to the functional architecture of synaptic connections (Banovic *et al.*, 2010;
26 Calahorro & Ruiz-Rubio, 2012; Chubykin *et al.*, 2007; Hu *et al.*, 2012; Hunter *et al.*, 2010;
27 Maglioni *et al.*, 2022; Sudhof, 2008; Sun *et al.*, 2011; Sun *et al.*, 2023; Tabuchi *et al.*, 2007;
28 Tu *et al.*, 2015; Varoqueaux *et al.*, 2006; Xing *et al.*, 2014).

29 Despite much investigation, however, several key questions about Nlgn function remain
30 unaddressed. Possibly the most important of these questions regards the observation
31 that different Nlgn isoforms, despite a high degree of sequence similarity, perform
32 largely non-overlapping distinct functions in the same neurons. How are different Nlgn
33 targeted to distinct synapses where they perform different roles? This question
34 represents an intriguing cell biological challenge given that Nlgn are postsynaptic, and
35 each neuron may receive inputs from thousands of neurons using the whole range of
36 neurotransmitter types. Since Nlgn interact with synapse-specific molecules at both the
37 post-synaptic (on the same cell) and pre-synaptic side (with molecules from the
38 projecting neuron), E/I specificity could be conferred to various Nlgn by intra- and/or
39 extra-cellular mechanisms. For example, Nlgn2 is primarily localized to inhibitory
40 synapses and Nlgn2 loss-of-function results in impaired inhibitory but not excitatory

1 synaptic transmission (Chanda *et al*, 2017; Chubykin *et al*, 2007; Gibson *et al*, 2009;
2 Liang *et al*, 2015; Poulopoulos *et al*, 2009; Zhang *et al*, 2015). Intracellularly, Nlgn2
3 binds to the inhibitory synapse-specific molecules gephyrin, collybistin, GARLH3, and
4 GARLH4, which are plausible candidates to recruit Nlgn2 to inhibitory synapses
5 (Poulopoulos *et al*, 2009; Yamasaki *et al*, 2017). However, the intracellular domains of
6 different Nlgn proteins are highly conserved, which argues against a strong contribution of
7 intracellular interaction partners as a mechanism of E/I specificity. On the extracellular
8 side facing pre-synaptic terminals, several molecules are also known to bind to Nlgn proteins.
9 The best characterized Nlgn interacting proteins are the three Nrns (Nrnx1-3), each of
10 which is expressed in hundreds of alternatively spliced variants (Treutlein *et al*, 2014).
11 With this impressive possibility of combinations, it is conceivable that specific "Nrnx
12 codes" could decorate different classes of synapses (Aoto *et al*, 2015; Dai *et al*, 2019;
13 Dai *et al*, 2021). More recently, the extracellular MDGA proteins have been described
14 as Nlgn regulators by binding to Nlgn proteins in competition with Nrns (Connor *et al*, 2019;
15 Lee *et al*, 2013; Tanaka *et al*, 2012). Crystal structures of MDGA1/Nlgn1 and
16 MDGA1/Nlgn2 complexes revealed that two N-terminal Ig domains of MDGA1 straddle
17 the Nlgn1 or Nlgn2 homodimer, such that each Nlgn homodimer binds to two MDGA1
18 molecules (Connor *et al*, 2016; Gangwar *et al*, 2017; Kim *et al*, 2017; Lee *et al*, 2013).
19 The binding of Nlgn proteins to MDGAs has been hypothesized to restrain Nlgn functions
20 (Elegheriet *et al*, 2017b; Pettem *et al*, 2013), but much about the mechanisms and
21 relative importance of this interaction is unknown. In summary, how Nlgn proteins target and
22 exert their functions at specific types of synapses remains a mystery.

23 Here, we begin to address some of these critical questions using expression of specific
24 Nlgn proteins and their mutants in cultured hippocampal neurons in which all Nlgn isoforms
25 were genetically deleted, with functional analyses performed by electrophysiology and
26 imaging. This approach reduces the complexity of potential interactions among different
27 Nlgn isoforms that can be present in the same postsynaptic compartment and
28 elucidates the inherent functions of the single Nlgn molecules expressed in this system,
29 thereby simplifying functional interpretations.

1 **Results**

2 **Specific synaptic targeting is an inherent property of Nlgn1 and Nlgn2**

3 The co-existence of various Nlgn genes in synapses complicates the conclusions about a
4 particular Nlgn using conventional experimental approaches. We therefore sought to
5 reduce the complexity to a neuronal cell system that contains only a single Nlgn of
6 interest. To this end, we generated quadruple conditional knock-out (cKO) mice where
7 all 4 endogenous Nlgn genes are conditionally deleted upon expression of Cre
8 recombinase. Our experimental setup is illustrated in Fig. 1A and entails (i) the
9 generation of primary hippocampal cultures of postnatal day 0 (P0) mice, (ii) the
10 expression by lentiviral transduction of active Cre recombinase or inactive ΔCre
11 recombinase as a control, and (iii) the co-expression of a specific Nlgn construct. We
12 performed immunoblots on lysates from Nlgn1234 cKO hippocampal cultures infected
13 with lentiviral ΔCre or Cre (Fig. EV1A and B). Cre expression caused a substantial loss
14 of Nlgn1, Nlgn2, and Nlgn3 (~70%-75%). Nlgn4 is not significantly expressed in this
15 culture system (Chanda *et al.*, 2017; Hoon *et al.*, 2011; Varoqueaux *et al.*, 2006).

16 To investigate the localization of Nlgn1 and Nlgn2 (that are known to localize to
17 specifically to excitatory and inhibitory synapses, respectively (Graf *et al.*, 2004;
18 Poulopoulos *et al.*, 2009; Song *et al.*, 1999; Varoqueaux *et al.*, 2004)), in the absence of
19 any other Nlgn genes, we expressed N-terminally hemagglutinin (HA)-tagged, full-length
20 Nlgn1 or Nlgn2 under control of the Synapsin promoter in hippocampal neurons after
21 Cre-mediated deletion of all endogenous Nlgn genes (Fig. 1B). Co-labeling with excitatory
22 and inhibitory synapse markers allowed us to assess the specific targeting of Nlgn1 and
23 Nlgn2 by fluorescence imaging. We detected strong expression of the infected Nlgn1
24 and Nlgn2 on MAP2-positive dendrites in a punctate pattern (Fig. 1C-F). We also co-
25 stained HA with Homer1 or Gephyrin as markers of excitatory and inhibitory synapses,
26 respectively (Fig. 1C and 1E). Consistent with reports about endogenous Nlgn1 and
27 Nlgn2 (Song *et al.*, 1999; Varoqueaux *et al.*, 2004), we found that in the absence of
28 endogenous Nlgn genes, the majority of HA-Nlgn1 puncta were co-localized with Homer1,
29 representing ~60% of the observed puncta. In contrast, HA-Nlgn1 puncta showed little
30 co-localization with Gephyrin, accounting for only ~27% of the observed puncta. HA-
31 Nlgn2 puncta, conversely, predominantly co-localized with Gephyrin, with ~59% of the
32 puncta showing this co-localization. Only ~28% of HA-Nlgn2 puncta co-localized with
33 Homer1 (Fig. 1D and F). We also analyzed the colocalization of Homer1 and Gephyrin
34 to address synapse specificity at the confocal level. We found ~21% Homer1 co-
35 localization with Gephyrin and ~30% Gephyrin co-localization with Homer1 ([Fig. EV1C](#)
36 and D). However, the background of positive colocalization with the 'wrong' synapse is
37 high due to the insufficient imaging resolution for separating closely spaced synapses
38 and the significant impact of thresholding on apparent colocalizations. Although these
39 findings are limited by the resolution of confocal microscopy, they are consistent with

1 previous conclusions that Nlgn1 primarily targets excitatory synapses while Nlgn2
2 primarily targets inhibitory synapses, showing that Nlgn1 and Nlgn2 exhibit this
3 specificity even in the absence of other Nlgn.

4

5 **The Gephyrin-binding domain of Nlgn2 is necessary for its inhibitory synapse-
6 specific function but does not confer inhibitory synapse specificity**

7 To investigate the molecular mechanisms targeting Nlgn2 to inhibitory synapses, we
8 generated Nlgn2 constructs with a truncation of the intracellular domain (Nlgn2-GPI)
9 and a chimeric Nlgn2 construct whose intracellular domain was switched with the
10 corresponding Nlgn1 sequence (Fig. 2A). We then expressed the constructs in our
11 Nlgn1234 cKO hippocampal neuron system. Cell surface staining of Nlgn2-GPI and
12 Nlgn2-Nlgn1 constructs in the Cre-infected neurons confirmed proper surface
13 localization, indicating that the introduced mutations do not interfere with protein
14 synthesis and processing in the secretory pathway (Fig. EV2A). Remarkably, co-
15 labeling with antibodies against the inhibitory synapse protein Gephyrin revealed that
16 both constructs localized to inhibitory synapses, but Nlgn2-Nlgn1 exhibited a higher
17 degree of localization with Gephyrin compared to Nlgn2-GPI (Fig. EV2B), and
18 expression levels no significant change (Fig. EV2C).

19 Next, we assessed the synaptic function of the Nlgn2 constructs using electrophysiology.
20 As expected, Cre-infected Nlgn1234 cKO hippocampal neurons exhibited a ~50%
21 decrease of evoked GABA-mediated inhibitory postsynaptic currents (IPSC) compared
22 to ΔCre-EGFP infected cultures (Fig. 2B and C), consistent with previous findings
23 (Chanda *et al.*, 2017; Gan & Sudhof, 2020). Expression of full-length Nlgn2 resulted in a
24 full rescue of the GABA-mediated IPSCs, demonstrating that Nlgn2 is the main Nlgn
25 isoform responsible for the inhibitory synapse phenotype observed with Nlgn1234
26 deletions (Fig. 2B and C). Intriguingly, expression of Nlgn2-GPI, i.e. Nlgn2 without an
27 intracellular domain, failed to rescue the phenotype (Fig. 2B and C), revealing that
28 Nlgn2 function for inhibitory synapses requires an intracellular domain presumably due
29 to the absence of synaptic targeting motifs in the GPI-anchor domain and the impact of
30 membrane anchoring on protein trafficking and synaptic recruitment. Given the
31 sequence similarity between the intracellular domains of Nlgn despite their different
32 synaptic functions, we assessed the function of a chimeric Nlgn2 with an intracellular
33 domain of Nlgn1. Consistent with previous results (Nguyen *et al.*, 2016), the Nlgn2-
34 Nlgn1 construct could also rescue the GABA-mediated IPSC phenotype in Nlgn1234
35 cKO neurons (Fig. 2B and C). Thus, the intracellular Nlgn2 domain is necessary for
36 inhibitory synapse function but does not confer specificity.

37 To further understand how Nlgn might function at synapses, we aligned Nlgn1 and
38 Nlgn2 intracellular sequences and confirmed that both Nlgn1 and Nlgn2 contain a highly
39 conserved Gephyrin-binding sequence (Fig. 3A), even though Nlgn1 is primarily

localized to excitatory synapses and has no function in inhibitory synapses (Chanda et al., 2017; Song et al., 1999; Zhang et al., 2015). This raised the question whether the Gephyrin-binding sequence is responsible for the Nlgn1 and Nlgn2 intracellular domain rescue of Nlgn2 function. To address this question, we deleted the entire 15 amino acid-long Gephyrin-binding sequence from the Nlgn2-Nlgn1 construct or introduced the Y770A point mutation which was shown to prevent Nlgn2 binding to Gephyrin by blocking the phosphorylation of this residue (Giannone et al., 2013; Poulopoulos et al., 2009) (Fig. 3B). Unexpectedly, expression of Nlgn2-Nlgn1Y770A construct fully rescued the IPSC phenotype, whereas the construct with the deletion of the entire Gephyrin-binding sequence (Nlgn2-Nlgn1 DelGeph) did not rescue (Fig. 3C and D). Again, we confirmed that the expressed constructs are properly transported to the cell surface by neuronal surface staining (Fig. EV2D). In line with our electrophysiology data, co-labeling with Gephyrin antibodies showed that the Nlgn2-Nlgn1 Y770A mutant displayed a greater degree of co-localization with Gephyrin than the Nlgn2-Nlgn1DelGeph mutant (Fig. EV2E), and expression levels no significant change (Fig. EV2F). These data show that the Gephyrin-binding sequence is critical for proper Nlgn2 function in inhibitory synapses but that either the interaction of Nlgn2 with Gephyrin alone may not be functionally necessary or that the Gephyrin interaction mediated by Y770 phosphorylation may be less relevant in a cellular context than *in vitro*.

20

21 **An intracellular sequence adjacent to the Gephyrin-binding region is necessary 22 for Nlgn2 inhibitory function**

Given the relative brevity of the intracellular Nlgn sequence, we set out to map the function of other intracellular Nlgn2 regions more comprehensively. To this end, we constructed a series of expanding Nlgn2 deletion constructs: Nlgn2-mt1 (Nlgn2 PDZ domain with the Nrxn PDZ domain) to test whether PSD95 and S-SCAM interaction with the Nlgn2 PDZ domain affects Nlgn2 inhibitory function; Nlgn2-mt2 (delete proline-rich domain) to test whether collybistin binding with the Nlgn2 proline-rich domain affects Nlgn2 inhibitory function; Nlgn2-mt3 (delete a 21-residue before the gephyrin binding domain); Nlgn2-mt4 and Nlgn2-mt5 are deleted large part of Nlgn2 except gephyrin binding domain (Fig. 4A and B). All constructs were confirmed to be localized to the neuronal cell surface (Fig. EV3A). First, we assessed the specificity of the PDZ domain using the Nlgn2-mt1 construct and collybistin domain using the Nlgn2-mt2 construct and found that this construct fully rescued the IPSC phenotype (Fig. 4C and D). We then tested Nlgn2-mt5 and Nlgn2-mt4, which proved to abolish the Nlgn2 function (Fig. 4C and D). Subsequent smaller deletions demonstrated that a 21-residue was necessary for the Nlgn2 function in addition to the previously identified Gephyrin interacting domain (Fig. 4C and D). No interactor is known for this sequence, suggesting that other

1 intracellular mechanisms in addition to gephyrin binding enable the inhibitory synapse
2 function of Nlgn2.

3

4 **The extracellular domain of Nlgn2 is required for inhibitory synapse function**

5 So far, we could establish that the intracellular domain of Nlgn2 is necessary for its
6 function in GABAergic synaptic transmission but that, at the same time, the Nlgn1
7 intracellular domain functionally substituted for the intracellular domain of Nlgn2. Thus,
8 the Nlgn2 intracellular domain does not determine its inhibitory synapse specificity.
9 Therefore, we asked whether Nlgn2's intracellular domain would be sufficient to recruit
10 Nlgn1 to function in GABAergic neurotransmission and created a Nlgn1-Nlgn2 construct
11 consisting of extracellular Nlgn1 and intracellular Nlgn2 domains (Fig. 5A).
12 Electrophysiological recordings showed that the Nlgn1-Nlgn2 chimeric construct was
13 unable to rescue the IPSC phenotype in Nlgn1-4 cKO neurons (Fig. 5B and C). Again,
14 we confirmed that Nlgn1-Nlgn2 properly localizes to the cell surface (Fig. EV2A). This
15 observation suggests that the extracellular domain of Nlgn2 plays a crucial role in
16 determining the specificity of Nlgn2 function in GABAergic synaptic transmission.

17

18 **Nlgn2 binding to MDGAs does not confer inhibitory synapse specificity to Nlgn2**

19 To examine what extracellular sequences mediate the inhibitory synapse function of
20 Nlgn2, we constructed a series of Nlgn2 variants with informative mutations in the
21 extracellular domain. We introduced into Nlgn2 a series of 5 point mutations
22 (Q370A/E372A/L374A/N375A/D377A) that are predicted to abolish Nrxn binding to
23 Nlgn2 based on previous results for Nlgn1 (Ko *et al.*, 2009), and a second set of 3 point
24 mutations (F433A/M434A/W438A) that correspond to Nlgn1 mutations which block
25 dimerization (Ko *et al.*, 2009). Unfortunately, these two sets of Nlgn2 mutations
26 prevented surface transport of Nlgn2, suggesting that they may hinder proper folding of
27 Nlgn2, which limited their usefulness (Fig. EV3B and C).

28 Recently the cell-adhesion molecules MDGA1 and MDGA2 were shown to compete
29 with Nrxns for binding to Nlgn2 (Connor *et al.*, 2016; Gangwar *et al.*, 2017; Kim *et al.*,
30 2017; Lee *et al.*, 2013). Crystal structures of the MDGA1/Nlgn2 complex provided
31 critical insights into this interaction, showing that the two N-terminal Ig domains of
32 MDGA1 bind to the Nlgn2 homodimer (Elegheriet *et al.*, 2017b; Gangwar *et al.*, 2017;
33 Kim *et al.*, 2017). To interrogate whether the interaction of MDGAs with the extracellular
34 domain of Nlgn2 confers synaptic specificity, we generated a Nlgn2 mutant (Nlgn2-
35 MDGA1mt) containing three point mutations H278A, D362K, E372K that were
36 previously shown to interfere with MDGA1 binding (Fig. 5D) (Gangwar *et al.*, 2017). The
37 Nlgn2-MDGA1mt construct properly localized to the neuronal surface and co-localized
38 with Gephyrin puncta (Fig. EV2A and B). In line with these findings, functional rescue

1 experiments revealed that the Nlgn2-MDGA1mt construct fully retained the ability of
2 Nlgn2 to rescue the IPSC impairment of Nlgn1234 cKO neurons (Fig. 5E and F). These
3 data suggest that MDGA1 does not directly suppress the inhibitory function of Nlgn2 in
4 synapses. This finding is consistent with recent work showing that MDGA1 targets APP,
5 but not Nlgn2, in hippocampal CA1 GABAergic neural circuits (Kim *et al*, 2022).

6

7 **The extracellular domain of Nlgn1 is sufficient for the excitatory synapse**
8 **specificity and function of Nlgn1**

9 Next, we asked whether the domain requirements we observed for Nlgn2 also apply to
10 other Nlgn. Therefore, we turned to Nlgn1 that is known to function exclusively in
11 excitatory synapses (Chanda *et al.*, 2017; Chubykin *et al.*, 2007; Gan & Sudhof, 2020;
12 Ko *et al.*, 2009; Song *et al.*, 1999) using equivalent experiments with Nlgn1234 cKO
13 hippocampal neurons expressing Cre-EGFP. As expected, we observed a significant
14 decrease in both AMPAR- and NMDAR-mediated excitatory synaptic responses when
15 we compared Cre-infected with ΔCre-infected neurons (Fig. 6B-D) (Chanda *et al.*, 2017;
16 Gan & Sudhof, 2020). The phenotype was more pronounced in NMDAR responses (~63%
17 decrease) compared to AMPAR responses (~39% decrease) (Fig. 6B and C), which is
18 consistent with previous findings (Chanda *et al.*, 2017; Gan & Sudhof, 2020).

19

20 To investigate Nlgn1 function, we performed rescue expression experiment with various
21 Nlgn1 variants (Fig. 6A). As expected, the excitatory synaptic phenotype could be fully
22 restored by full-length Nlgn1 expression (Fig. 6B-D). However, in contrast to what we
23 had observed for Nlgn2, the Nlgn1-GPI construct (Nlgn1 without an intracellular domain)
24 also rescued the excitatory synapse phenotype. Consistent with a lack of importance of
25 the intracellular Nlgn1 domain, a Nlgn2-Nlgn1 construct was unable to rescue the
26 glutamatergic synaptic phenotype (Fig. 6B-D). Importantly, we confirmed the surface
27 expression Nlgn1-GPI and Nlgn2-Nlgn1. Co-localization of the constructs with Homer1
28 revealed that a larger fraction of Nlgn1-GPI, and a smaller fraction of Nlgn2-Nlgn1 were
29 co-localized with Homer1 (Fig. EV4A and B), and expression levels no significant
30 change (Fig. EV4C). **We also found Nlgn1-Nlgn2 is sufficient for the glutamatergic**
31 **synaptic transmission function of Nlgn1, but Nlgn2-WT doesn't (Fig. EV5).** These
32 findings demonstrate that - unlike for Nlgn2 - the extracellular domain of Nlgn1 is
33 sufficient for Nlgn1 function and also confers specificity to excitatory synaptic
34 transmission.

35

36 **Nrxn- and MDGA1-binding and dimerization of Nlgn1 are not required for**
37 **glutamatergic synaptic transmission**

1 The observation that the extracellular domain of Nlgn1 is critical for its excitatory
2 synapse function suggests that its physical interaction with presynaptic binding partners
3 is important. Known Nlgn1-binding partners include Nrns and MDGAs. To test the
4 necessity of these interactions, we generated Nlgn1 variants that are unable to bind
5 Nrns and MDGA1, respectively (Arac *et al*, 2007; Ko *et al.*, 2009). To more generally
6 assess the importance of extracellular Nlgn1 interactions, we also generated a Nlgn1
7 variant that is unable to dimerize (Fig. 7A). All constructs were appropriately expressed
8 on the neuronal surface (Fig. EV4D). Also, and remarkably, all constructs exhibited a
9 high degree of co-localization with Homer1 (Fig. EV4E), and expression levels no
10 significant change (Fig. EV4F). In concordance with these results, electrophysiological
11 measurements demonstrated that all three constructs fully rescued the excitatory
12 phenotype of Nlgn1^{-/-} neurons (Fig. 7B-D). These results suggest the surprising
13 notion that neither Nrns- nor MDGA1-binding and not even dimerization of Nlgn1 is
14 necessary for Nlgn1 function despite the functional necessity of its extracellular, but not
15 its intracellular domain.

1 **Discussion**

2 Nlgn1 and Nlgn2 function selectively in glutamatergic excitatory and GABAergic
3 inhibitory synapses, respectively, but how their synapse specificity is determined
4 remains unclear. In this study, we sought to investigate the mechanisms that confer this
5 intriguing synapse specificity onto Nlgn1 and Nlgn2 and to understand how two closely
6 related proteins can possess such contrasting functions. To eliminate the potentially
7 confounding effects of other Nlgn proteins that may heterodimerize with exogenously
8 expressed Nlgn proteins or otherwise influence a specific Nlgn under investigation, we here
9 resorted to a reductionistic approach that employs a primary neuronal culture system
10 lacking endogenous Nlgn proteins. Specifically, we used as a general substrate of functional
11 analyses neurons that lack all four Nlgn proteins, in which we then expressed a specific Nlgn
12 mutant. Surprisingly, we found that different molecular mechanisms guide Nlgn1 and
13 Nlgn2 function in this system. Our results allow us to draw five main conclusions.

14 First, deletion of all four Nlgn proteins results in a major dysfunction of both GABAergic and
15 glutamatergic synapses, demonstrating that neuronal Nlgn proteins are crucial for proper
16 synaptic transmission. These results are consistent with previous findings using
17 Nlgn123 cKO and Nlgn1234 cKO mice (Chanda *et al.*, 2017; Gan & Sudhof, 2020). Our
18 findings further corroborate the notion that Nlgn1 is important for glutamatergic and
19 Nlgn2 for GABAergic neurotransmission since Nlgn1 could selectively rescue the
20 glutamatergic defect and Nlgn2 the GABAergic defect of Nlgn1234 cKO neurons.
21 Moreover, Nlgn1 molecules were primarily targeted to Homer1-positive excitatory
22 synapses and Nlgn2 to Gephyrin-positive inhibitory synapses.

23 Second, Nlgn2's function at inhibitory synapses requires its intracellular domain. Given
24 this finding, interactions mediated by the intracellular domain would represent an
25 attractive mechanism to target Nlgn2 to GABAergic synapses given the many inhibitory
26 synapse-specific scaffolding proteins that are known to bind to the Nlgn2 cytoplasmatic
27 domain (Poulopoulos *et al.*, 2009; Tyagarajan *et al.*, 2011). Unexpectedly, however, the
28 Nlgn2 intracellular domain was unable to confer onto Nlgn2 its GABAergic synapse
29 specificity since the Nlgn1 intracellular domain was fully capable of substituting for the
30 Nlgn2 intracellular domain. A conspicuous similarity between Nlgn1 and Nlgn2 is the
31 Gephyrin-binding sequence that is equally present in the Nlgn1 and Nlgn2 cytoplasmic
32 domain despite the fact that Nlgn1 exclusively functions in excitatory synapses lacking
33 Gephyrin. Gephyrin is a key postsynaptic scaffolding protein at GABAergic synapses
34 that enables the recruitment of GABA_A receptors to synapses (Choii & Ko, 2015;
35 Tyagarajan & Fritschy, 2014). Importantly, we found that the Gephyrin-interacting
36 domain is necessary for Nlgn2 function, suggesting that recruitment by Gephyrin is
37 indeed important. However, Gephyrin may not be the only important Nlgn2 binding
38 partner. A Nlgn2 variant that carries the Y770A mutation, previously shown to disrupt
39 Gephyrin binding (Giannone *et al.*, 2013; Poulopoulos *et al.*, 2009), was still fully

1 functional. This finding suggests that potentially other co-factors may stabilize the
2 Gephyrin-Nlgn2 interaction overcoming the Y770A mutation. A previous study also
3 showed an only partial functional impairment of Nlgn2 by the Y770A mutation (Nguyen
4 *et al.*, 2016). However, in this paper the deletion of the entire Gephyrin binding
5 sequence also only partly impaired Nlgn2 function whereas in our experiments such a
6 deletion was functional deleterious. Overall, these results prompted us to look for
7 additional cytosolic Nlgn2 sequences that are important for Nlgn2 function. Through
8 targeted mutagenesis, we identified a new sequence of **21-residue** that is just as critical
9 as the better characterized Gephyrin-binding sequence and may represent a binding
10 surface for additional postsynaptic proteins at GABAergic synapses. Of note, the two
11 amino acid residues K749 and R750 were shown to be ubiquitinated and methylated,
12 respectively (Guo *et al*, 2014; Wagner *et al*, 2012).

13 Third, we found that different Nlgnns use distinct functional mechanisms at their target
14 synapses. Whereas Nlgn2 requires its intracellular domain for enabling inhibitory
15 synaptic connections, Nlgn1 -consistent with previous results (Jiang *et al*, 2017; Wu *et*
16 *al*, 2019)- does not. This may be our conceptually most intriguing result: Despite the fact
17 that Nlgn1 and Nlgn2 are both enabling synapse function, albeit at different types of
18 synapses, their mechanisms of action differ critically.

19 Fourth, the extracellular but not the intracellular domain of Nlgn1 and Nlgn2 determines
20 their specificity for glutamatergic and GABAergic synapses, respectively. The
21 Intracellular domain of Nlgn2 (but intriguingly not of Nlgn1) is necessary for synaptic
22 localization and its "specific" recruitment to synapses. Chimeric Nlgn2-Nlgn1 molecules
23 enabled GABAergic synaptic transmission, but not glutamatergic, while chimeric Nlgn1-
24 Nlgn2 molecules mediated glutamatergic, but not GABAergic synaptic transmission.
25 The specificity for glutamatergic vs. GABAergic synapses is dictated by the Nlgn1, and
26 Nlgn2 extracellular domains, respectively. Nrxns are well-studied pre-synaptic binding
27 partners of Nlgnns and thus could provide synapse specificity. However, we found that
28 Nlgn1 variants unable to bind Nrxns still rescued the excitatory phenotypes as reported
29 previously (Ichtchenko *et al.*, 1995; Ichtchenko *et al.*, 1996; Jiang *et al.*, 2017; Ko *et al.*,
30 Sudhof, 2017; Wu *et al.*, 2019). These results suggest that Nlgnns function via
31 interactions with other binding partners in addition to Nrxns. Indeed, recently MDGA
32 proteins have been identified as Nlgn interaction partners, binding through their Ig1-Ig2
33 domains to the lobes of the Nlgn extracellular dimer at sites overlapping with the Nrxn
34 binding interface (Elegheriet *et al*, 2017a; Gangwar *et al.*, 2017; Kim *et al.*, 2017). They
35 thus emerge as candidates that may provide synapse specificity for Nlgnns. Remarkably,
36 however, we found that mutant Nlgn1 predicted to lack MDGA binding was fully able to
37 rescue Nlgn1 function, indicating that this class of interaction is also not providing
38 specificity. Additionally, *in vivo* experiments show that MDGA1 targets APP, but not
39 Nlgn2, in hippocampal CA1 GABAergic neural circuits to regulate GABAergic synaptic
40 transmission (Kim *et al.*, 2022). In addition to MDGAs, at least Nlgn3 has been shown to

1 bind to PTPRD (Yoshida *et al*, 2021), which in turn binds to neurexins (Han *et al*, 2018),
2 suggesting a possible synapse maintenance mechanism involving multiple trans-
3 synaptic interactions.

4 Finally, we conclude that Nlgn1 may be acting as a monomer in regulating synaptic
5 transmission and that no binding event that involves signal transduction mediated by
6 dimerization plays a role in Nlgn1's specificity. Mutations disrupting Nlgn1 dimerization
7 did not impair Nlgn1 function in our hippocampal cell assay. Intriguingly, a previous
8 study showed that Nlgn1 overexpression enhances both NMDAR- and AMPAR- EPSCs
9 in neurons, even when dimerization is disrupted (Ko *et al.*, 2009).

10 Our studies also raise new questions. With the conclusion that extracellular
11 mechanisms must be responsible for functional specificity of Nlgns, but neither Nrnx nor
12 MDGA interactions are themselves sufficient to account for the specificity of Nlgns,
13 there must be other thus-far unidentified proteins present at excitatory and inhibitory
14 pre-synaptic compartments that interact with Nlgns. In the case of Nlgn2, the
15 intracellular domain is critical for synaptic function, but its exact role continues to be
16 unclear. For example, Nlgn2 activation by an extracellular signal could stimulate a
17 defined signal-transduction cascade, akin to a conventional receptor/ligand-induced
18 signaling pathway. Unraveling these signaling mechanisms will contribute to a
19 comprehensive understanding of the molecular pathways governing Nlgn-mediated
20 synaptic processes. These questions are crucial for a general understanding of the
21 diversity of Nlgns functions. Detailed molecular, genetic, and biochemical approaches
22 may lead to a better insight into these questions.

23

24

25 **Methods**

26 **Mouse breeding and husbandry**

27 All animal experiments were performed with male and female newborn mice according
28 to institutional guidelines and approved by the Administrative Panel on Laboratory
29 Animal Care of Stanford University School of Medicine ([Protocol ID: 18846](#)). A detailed
30 description of generating Nlgn1234 cKO mice is describe in the previous study (Wu *et*
31 *al.*, 2019). All experiments except for Figure EV1, were performed in a “blinded” fashion
32 (i.e., the experimenter was unaware of whether a sample represented a test or control
33 sample).

34 **Plasmids and Lentivirus preparation**

35 All plasmids were in a pFSW67 backbone and used the human synapsin promoter, for
36 all neuroligin added an N-terminal HA peptide fused to the mature coding sequence.
37 Lentivirus were prepared as described previously (Chanda *et al.*, 2017). Briefly, the

1 lentiviral expressing vectors (12 µg) were co-transfected with three helper plasmids
2 (pRSV-REV (4µg), pMDLg/pRRE (8µg), and VSV-G (6µg)) into HEK293T cells cultured
3 in T-75 flasks using calcium phosphate transfection. After a complete medium exchange
4 at 7h, supernatants were subsequently collected at 48h, filtered via 0.45 µm filter and
5 ultracentrifuged at 64000 ×g for 2h. Pellets were resuspended in MEM and stored at -80
6 °C before use. All viruses used in this paper are as below:
7 Lenti-Syn-ΔCre-EGFP
8 Lenti-Syn-Cre-EGFP
9 Lenti-Syn-HA-Nlgn1-WT (Nlgn1-wild-type)
10 Lenti-Syn-HA-Nlgn1-GPI (We deleted all transmembrane regions and cytoplasmic
11 sequences of Nlgn1 and attaches its extracellular domains to the membrane using a
12 GPI-anchor)
13 Lenti-Syn-HA-Nlgn1-Nlgn2 (We made the extracellular domain of Nlgn1 transplanted
14 onto Nlgn2 intercellular.)
15 Lenti-Syn-HA-Nlgn1-Nrxnmt (Nlgn1 with Nrxn binding site mutant was generated by
16 making previously described mutations Q395A/E397A/L399A/N400A/D402A (Arac *et al.*,
17 2007).)
18 Lenti-Syn-HA-Nlgn1-dimmt (Nlgn1 dimerization mutant was generated by making
19 previously described mutations F458A/M459A/W463A (Arac *et al.*, 2007; Ko *et al.*,
20 2009).)
21 Lenti-Syn-HA-Nlgn1-MDGA1mt (We aligned the Nlgn1 and Nlgn2 sequences, made the
22 Nlgn1 with MDGA1 binding site mutations H303A/D387K/E397K.)
23 Lenti-Syn-HA-Nlgn2-WT (Nlgn2-wild-type)
24 Lenti-Syn-HA-Nlgn2-GPI (We deleted all transmembrane regions and cytoplasmic
25 sequences of Nlgn2 and attaches its extracellular domains to the membrane using a
26 GPI-anchor.)
27 Lenti-Syn-HA-Nlgn2-Nlgn1 (We made extracellular domain of Nlgn2 transplanted onto
28 Nlgn1 intercellular.)
29 Lenti-Syn-HA-Nlgn2-Nrxnmt (We aligned the Nlgn1 and Nlgn2 sequences, made the
30 Nlgn2 with Nrxn binding site mutations Q370A/E372A/L374A/N375A/D377A.)
31 Lenti-Syn-HA-Nlgn2-dimmt (We aligned the Nlgn1 and Nlgn2 sequences, made the
32 Nlgn2 dimerization mutations F433A/M434A/W438A.)
33 Lenti-Syn-HA-Nlgn2-MDGA1mt (Nlgn2 with MDGA1 binding site mutant was generated
34 by making previously described mutations H278A/D362K/E372K (Gangwar *et al.*,
35 2017).)

1 Lenti-Syn-HA-Nlgn2mt1 (We replaced the Nlgn2-PDZ domain HSTTRV with Nrxx-PDZ
2 domain KKNKDKEYYV.)
3 Lenti-Syn-HA-Nlgn2mt2 (We deleted Nlgn2 intracellular sequences
4 PPPPPPPPSLHPFPPPPPTATSHNNTLPHP.)
5 Lenti-Syn-HA-Nlgn2mt3 (We deleted Nlgn2 intracellular sequences
6 EEELVSLQLKRGGGVGADPAE.)
7 Lenti-Syn-HA-Nlgn2mt4 (We deleted Nlgn2 intracellular sequences
8 GSGSGVPGGGPLLPTAGRELPEEEELVSLQLKRGGGVGADPAE.)
9 Lenti-Syn-HA-Nlgn2mt5 (We deleted Nlgn2 intracellular sequences
10 GSGSGVPGGGPLLPTAGRELPEEEELVSLQLKRGGGVGADPAE
11 and PPPPPPPPSLHPFPPPPPTATSHNNTLPHP.)
12 Lenti-Syn-HA-Nlgn2-Nlgn1 Y-A (We made extracellular domain of Nlgn2 transplanted
13 onto Nlgn1 intercellular and made gephyrin binding point mutation as previously
14 described Y770A (Poulopoulos *et al.*, 2009).)
15 Lenti-Syn-HA-Nlgn2-Nlgn1 dele Geph (We deleted the whole Nlgn1 with gephyrin
16 binding domain sequences PDYTLALRRRAPDDVP)

17 **Neuronal culture and lentivirus infection**

18 Cell culture of hippocampal primary neurons from both male and female Nlgn1234 cKO
19 newborn (P0) mice was performed as described previously (Wang *et al*, 2022). Briefly,
20 dissected hippocampus was digested at 37 °C for 25 min with 10U/ml papain in HBSS
21 buffer, washed three times with plating medium (MEM supplemented with 0.5% glucose,
22 0.02% NaHCO₃, 0.1 mg/ml transferrin, 10% FBS, 2 mM L-glutamine, and 0.025% mg/ml
23 insulin), and then gently dissociated in plating medium, and filter with 70 µm cell strainer,
24 and seeded on Matrigel pre-coated coverslip placed inside 24-well plate. The day of
25 plating was considered as 0 days in vitro (DIV 0). After 24 h (DIV 1), 90% of the plating
26 medium was replaced with neuronal growth medium (Neurobasal supplemented with
27 0.5% glucose, 0.02% NaHCO₃, 0.1 mg/ml transferrin, 5% FBS, 2% B27 supplement,
28 and 0.5 mM L-glutamine), At DIV3, 50% of the medium was replaced with fresh growth
29 medium additionally supplemented with finally concertation 4 µM Ara-C. Cultured
30 hippocampal neurons were infected at DIV 4 with lentiviruses expressing ΔCre-EGFP or
31 Cre-EGFP and subsequently were infected at DIV 6 with lentiviruses expressing
32 different neuroligin constructs.

33 **Immunohistochemistry**

34 All solutions were made fresh and filtered via a 0.22 µm filter prior to staring
35 experiments. For HA surface-labeling experiments were performed as described
36 previously (Trotter *et al*, 2019). Briefly, primary neurons were first washed at room

1 temperature once with a normal Tyrode's bath solution, and then incubated for 20 min
2 with purified Mouse anti-HA monoclonal antibody (1:500; BioLegend, [Cat. #: 901501](#)) or
3 Rabbit anti-HA monoclonal antibody (1:500; Cell Signaling Technologies, [Cat. #: 3724S](#))
4 diluted in normal Tyrode's bath solution. Cultures were then gently washed three times
5 with normal Tyrode's bath solution, followed by fixation for 20 min at 4 °C with 4% PFA.
6 Following fixation, cultures were washed three times with Dulbecco's PBS (DPBS). For
7 surface labeling experiments (All the Nlgn constructs were all incubated live with an
8 anti-HA monoclonal antibody and then fixed and further processed) to be used for
9 conventional imaging, cultures were blocked for 1 h at room temperature with antibody
10 dilution buffer (ADB) without Triton x-100, which contains 5% normal goat serum diluted
11 in DPBS. Cultures were then labeled with Alexa Fluor-conjugated secondary antibody
12 (1:1000; Invitrogen) diluted in ADB for 1h at room temperature. Next for non-surface
13 labeling, cells were washed and permeabilized and blocked for 1 h with ADB with Triton
14 x-100, which contains 0.2% Triton x-100 and 5% normal goat serum diluted in DPBS.
15 Non-surface primary antibodies [Guinea pig anti-Gephyrin monoclonal antibody \(1:200, Synaptic Systems, Cat. #: 147318\)](#) or [Mouse anti-Gephyrin monoclonal antibody \(1:1000, Synaptic Systems, Cat. #: 147011\)](#)/ [Rabbit anti-Homer1 monoclonal antibody \(1:500, Millipore, Cat. #: ABN37\)](#) or [Guinea pig anti-Homer1 monoclonal antibody \(1:500, Synaptic Systems, Cat. #: 160005\)](#) /[Chicken anti-MAP2 monoclonal antibody \(1:1000, Encor, Cat. #: CPC-A-MAP2\)](#) were diluted in ADB, and cells were incubated
16 overbought at 4 °C or 2h at room temperature. Cultures were washed three times and
17 then incubated with either Alexa Fluor-conjugated secondary antibodies (1:1000;
18 Invitrogen) in ABD for 1h. Following three washed, coverslip for conventional imaging
19 were inverted onto glass microscope slides with Fluoromount-G Mounting medium
20 (Southern Biotech). In certain experiments, the number of cells analyzed was relatively
21 low, as indicated in Fig1D and 1F. Despite this, the observed effect size and the
22 consistency of the results suggest that the sample size was sufficient.

28 [Immunoblotting](#)

29 Hippocampal neurons in 24-well plates were lysed in RIPA buffer containing 150 mM
30 NaCl, 1% Triton X-100, 0.1% SDS, 25 mM Tris-HCl, pH 7.4, and Complete EDTA-Free
31 Protease Inhibitor Cocktail (Sigma Millipore). Lysates were incubated on ice for 30 min
32 and clarified by centrifugation at 14,000 g for 30 min at 4°C. Lysates were boiled in
33 sample buffer containing 1% β -mercaptoethanol at 42 °C for 30 min. Proteins were
34 analyzed by SDS-PAGE using 4%-20% Mini-Protean TGX precast gels (Bio-Rad).
35 Proteins were transferred onto nitrocellulose membranes for 7 min at 25 V using the
36 Trans-Blot Turbo transfer system (Bio-Rad). Membranes were blocked in 5% milk
37 diluted in TBST for 1 h at room temperature. Membranes were then incubated overnight
38 at 4°C with the following primary antibodies diluted in 5% BSA diluted in TBST solution:
39 [Mouse anti-Nlgn1 \(1:1000, Synaptic Systems, Cat. #: ab308451\)](#), [Mouse anti-Nlgn2](#)

1 (1:1000, Synaptic Systems, Cat. #: ab317510), Rabbit anti-Nlgn3 (639B, 1:500, T.C.S.
2 laboratory), and Rabbit anti-Tuj1 (1:1000, BioLegend, Cat. #: 802001) Membranes were
3 subsequently incubated for 1 h at room temperature with the following compatible
4 secondary antibodies (LI-COR), diluted 1:10,000 in blocking solution: IRDye 800LT
5 donkey anti-mouse or anti-Rabbit; IRDye 800CW donkey anti-mouse or anti-Rabbit.
6 Quantitative analysis was performed by a dual-channel infrared imaging system, an
7 **Odyssey Infrared Imager CLX**, and **Image Studio 5.2.5** software (LI-COR).

8 **Confocal image acquisition and analysis**

9 Serial confocal z-stack images were acquired using a Nikon confocal microscope
10 (A1RSi) with a 40× objective. Images were analyzed with by NIS-Elements AR analysis
11 software.

12 **Electrophysiology**

13 Electrophysiological recordings were performed from primary hippocampal culture
14 neurons plated on coverslip, which were placed in a recording chamber mounted on a
15 fixed stage inverted phase-contrast microscope (Olympus). Patch electrodes (3-5 MΩ)
16 were pulled from borosilicate glass capillary tubes (Warner Instruments) using a PC-10
17 pipette puller (Narishige). Whole-cell capacitance and series resistances were recorded
18 and compensated to >80%, and in addition, series resistances were less than two times
19 the tip resistance. The Tyrode's bath solution contained (in mM): 129 NaCl, 5 KCl, 2
20 CaCl₂, 1 MgCl₂, 0.01 glycine, 30 D-glucose and 25 HEPES, pH 7.2–7.4.

21 All recording under voltage-clamp model with a pipette solution containing (in mM): 135
22 CsCl, 10 HEPES, 10 EGTA, 2 Mg-ATP, 2 Na₂GTP, and 5 QX-314, pH 7.35 (adjusted
23 with CsOH). Presynaptic Action-potential for evoked synaptic responses were triggered
24 by 0.5-ms current (40-90 μA) injections through a local extracellular electrode (FHC
25 concentric bipolar electrode, Catalogue number CBAEC75) placed ~100 μm from the
26 soma of neurons recorded. Inhibitory synaptic currents were made in presence of 20 μM
27 CNQX and 50 μM APV to block AMPAR and NMDAR-mediated currents respectively.
28 GABAR-IPSCs were recorded at -60 mV and measured at the peak of the current.

29 Excitatory synaptic currents were made in presence of 100 μM picrotoxin to block
30 inhibitory currents and a small (10 nM) amount of TTX to reduced epileptiform activity.
31 AMPAR-EPSCs were recorded as the peak current (~2 ms window) at -70 mV and
32 NMDAR-EPSCs at +40 mV.

33 **Quantifications and statistical analyses**

34 Electrophysiological data were analyzed in Clampfit 10.7 (Molecular Devices). For
35 clarity, all stimulus were blanked and not shown in the figures. All data were shown as
36 means ± SEM, numbers of cells and batches analyzed are shown in the bars. Statistical
37 significance (*p<0.05; **p<0.01; ***p<0.001; ****p<0.0001, non-significant comparisons

1 are indicted as NS) was analyzed with Prism 9, GraphPad. Unpaired t test was used for
2 comparison between two groups. One-way ANOVA was used for comparison among
3 more than two groups.

4 **Data availability**

5 No data have been deposited to public repositories.

6 **Acknowledgements**

7 This study was supported by grant from the National Institute of Mental Health (NIMH)
8 (2R01MH092931 to M.W and T.C.S.)

Disclosure and competing interests statement

The authors declare no competing interest.

1 **REFERENCES**

- 2 Aoto J, Foldy C, Ilcus SM, Tabuchi K, Sudhof TC (2015) Distinct circuit-dependent
3 functions of presynaptic neurexin-3 at GABAergic and glutamatergic synapses. *Nat
4 Neurosci* 18: 997-1007
- 5 Arac D, Boucard AA, Ozkan E, Strop P, Newell E, Sudhof TC, Brunger AT (2007)
6 Structures of neuroligin-1 and the neuroligin-1/neurexin-1 beta complex reveal specific
7 protein-protein and protein-Ca²⁺ interactions. *Neuron* 56: 992-1003
- 8 Banovic D, Khorramshahi O, Owald D, Wichmann C, Riedt T, Fouquet W, Tian R, Sigrist
9 SJ, Aberle H (2010) Drosophila neuroligin 1 promotes growth and postsynaptic
10 differentiation at glutamatergic neuromuscular junctions. *Neuron* 66: 724-738
- 11 Bolliger MF, Pei J, Maxeiner S, Boucard AA, Grishin NV, Sudhof TC (2008) Unusually
12 rapid evolution of Neuroligin-4 in mice. *Proc Natl Acad Sci U S A* 105: 6421-6426
- 13 Budreck EC, Scheiffele P (2007) Neuroligin-3 is a neuronal adhesion protein at
14 GABAergic and glutamatergic synapses. *Eur J Neurosci* 26: 1738-1748
- 15 Calahorro F, Ruiz-Rubio M (2012) Functional phenotypic rescue of *Caenorhabditis
16 elegans* neuroligin-deficient mutants by the human and rat NLGN1 genes. *PLoS One* 7:
17 e39277
- 18 Chanda S, Hale WD, Zhang B, Wernig M, Sudhof TC (2017) Unique versus Redundant
19 Functions of Neuroligin Genes in Shaping Excitatory and Inhibitory Synapse Properties.
20 *J Neurosci* 37: 6816-6836
- 21 Choii G, Ko J (2015) Gephyrin: a central GABAergic synapse organizer. *Exp Mol Med*
22 47: e158
- 23 Chubykin AA, Atasoy D, Etherton MR, Brose N, Kavalali ET, Gibson JR, Sudhof TC
24 (2007) Activity-dependent validation of excitatory versus inhibitory synapses by
25 neuroligin-1 versus neuroligin-2. *Neuron* 54: 919-931
- 26 Connor SA, Ammendrup-Johnsen I, Chan AW, Kishimoto Y, Murayama C, Kurihara N,
27 Tada A, Ge Y, Lu H, Yan R et al (2016) Altered Cortical Dynamics and Cognitive
28 Function upon Haploinsufficiency of the Autism-Linked Excitatory Synaptic Suppressor
29 MDGA2. *Neuron* 91: 1052-1068
- 30 Connor SA, Elegheert J, Xie Y, Craig AM (2019) Pumping the brakes: suppression of
31 synapse development by MDGA-neuroligin interactions. *Curr Opin Neurobiol* 57: 71-80
- 32 Dai J, Aoto J, Sudhof TC (2019) Alternative Splicing of Presynaptic Neurexins
33 Differentially Controls Postsynaptic NMDA and AMPA Receptor Responses. *Neuron*
34 102: 993-1008 e1005
- 35 Dai J, Patzke C, Liakath-Ali K, Seigneur E, Sudhof TC (2021) GluD1 is a signal
36 transduction device disguised as an ionotropic receptor. *Nature* 595: 261-265
- 37 Elegheert J, Cvetkovska V, Clayton AJ, Heroven C, Vennekens KM, Smukowski SN,
38 Regan MC, Jia W, Smith AC, Furukawa H et al (2017a) Structural Mechanism for
39 Modulation of Synaptic Neuroligin-Neurexin Signaling by MDGA Proteins. *Neuron* 96:
40 242-244
- 41 Elegheert J, Cvetkovska V, Clayton AJ, Heroven C, Vennekens KM, Smukowski SN,
42 Regan MC, Jia W, Smith AC, Furukawa H et al (2017b) Structural Mechanism for
43 Modulation of Synaptic Neuroligin-Neurexin Signaling by MDGA Proteins. *Neuron* 95:
44 896-913 e810

- 1 Gan KJ, Sudhof TC (2020) SPARCL1 Promotes Excitatory But Not Inhibitory Synapse
2 Formation and Function Independent of Neurexins and Neuroligins. *J Neurosci* 40:
3 8088-8102
- 4 Gangwar SP, Zhong X, Seshadrinathan S, Chen H, Machius M, Rudenko G (2017)
5 Molecular Mechanism of MDGA1: Regulation of Neuroligin 2:Neurexin Trans-synaptic
6 Bridges. *Neuron* 94: 1132-1141 e1134
- 7 Giannone G, Mondin M, Grillo-Bosch D, Tessier B, Saint-Michel E, Czondor K, Sainlos
8 M, Choquet D, Thoumine O (2013) Neurexin-1beta binding to neuroligin-1 triggers the
9 preferential recruitment of PSD-95 versus gephyrin through tyrosine phosphorylation of
10 neuroligin-1. *Cell Rep* 3: 1996-2007
- 11 Gibson JR, Huber KM, Sudhof TC (2009) Neuroligin-2 deletion selectively decreases
12 inhibitory synaptic transmission originating from fast-spiking but not from somatostatin-
13 positive interneurons. *J Neurosci* 29: 13883-13897
- 14 Graf ER, Zhang X, Jin SX, Linhoff MW, Craig AM (2004) Neurexins induce
15 differentiation of GABA and glutamate postsynaptic specializations via neuroligins. *Cell*
16 119: 1013-1026
- 17 Guo A, Gu H, Zhou J, Mulhern D, Wang Y, Lee KA, Yang V, Aguiar M, Kornhauser J, Jia
18 X et al (2014) Immunoaffinity enrichment and mass spectrometry analysis of protein
19 methylation. *Mol Cell Proteomics* 13: 372-387
- 20 Han KA, Ko JS, Pramanik G, Kim JY, Tabuchi K, Um JW, Ko J (2018) PTPsigma Drives
21 Excitatory Presynaptic Assembly via Various Extracellular and Intracellular Mechanisms.
22 *J Neurosci* 38: 6700-6721
- 23 Hoon M, Soykan T, Falkenburger B, Hammer M, Patrizi A, Schmidt KF, Sassoe-
24 Pognetto M, Lowel S, Moser T, Taschenberger H et al (2011) Neuroligin-4 is localized to
25 glycinergic postsynapses and regulates inhibition in the retina. *Proc Natl Acad Sci U S A*
26 108: 3053-3058
- 27 Hu Z, Hom S, Kudze T, Tong XJ, Choi S, Aramuni G, Zhang W, Kaplan JM (2012)
28 Neurexin and neuroligin mediate retrograde synaptic inhibition in *C. elegans*. *Science*
29 337: 980-984
- 30 Hunter JW, Mullen GP, McManus JR, Heatherly JM, Duke A, Rand JB (2010)
31 Neuroligin-deficient mutants of *C. elegans* have sensory processing deficits and are
32 hypersensitive to oxidative stress and mercury toxicity. *Dis Model Mech* 3: 366-376
- 33 Ichtchenko K, Hata Y, Nguyen T, Ullrich B, Missler M, Moomaw C, Sudhof TC (1995)
34 Neuroligin 1: a splice site-specific ligand for beta-neurexins. *Cell* 81: 435-443
- 35 Ichtchenko K, Nguyen T, Sudhof TC (1996) Structures, alternative splicing, and neurexin
36 binding of multiple neuroligins. *J Biol Chem* 271: 2676-2682
- 37 Jamain S, Quach H, Betancur C, Rastam M, Colineaux C, Gillberg IC, Soderstrom H,
38 Giros B, Leboyer M, Gillberg C et al (2003) Mutations of the X-linked genes encoding
39 neuroligins NLGN3 and NLGN4 are associated with autism. *Nat Genet* 34: 27-29
- 40 Jiang M, Polepalli J, Chen LY, Zhang B, Sudhof TC, Malenka RC (2017) Conditional
41 ablation of neuroligin-1 in CA1 pyramidal neurons blocks LTP by a cell-autonomous
42 NMDA receptor-independent mechanism. *Mol Psychiatry* 22: 375-383
- 43 Kim J, Kim S, Kim H, Hwang IW, Bae S, Karki S, Kim D, Ogelman R, Bang G, Kim JY et
44 al (2022) MDGA1 negatively regulates amyloid precursor protein-mediated synapse
45 inhibition in the hippocampus. *Proc Natl Acad Sci U S A* 119

- 1 Kim JA, Kim D, Won SY, Han KA, Park D, Cho E, Yun N, An HJ, Um JW, Kim E et al
2 (2017) Structural Insights into Modulation of Neurexin-Neuroligin Trans-synaptic
3 Adhesion by MDGA1/Neuroligin-2 Complex. *Neuron* 94: 1121-1131 e1126
- 4 Ko J, Zhang C, Arac D, Boucard AA, Brunger AT, Sudhof TC (2009) Neuroligin-1
5 performs neurexin-dependent and neurexin-independent functions in synapse
6 validation. *EMBO J* 28: 3244-3255
- 7 Lee K, Kim Y, Lee SJ, Qiang Y, Lee D, Lee HW, Kim H, Je HS, Sudhof TC, Ko J (2013)
8 MDGAs interact selectively with neuroligin-2 but not other neuroligins to regulate
9 inhibitory synapse development. *Proc Natl Acad Sci U S A* 110: 336-341
- 10 Liang J, Xu W, Hsu YT, Yee AX, Chen L, Sudhof TC (2015) Conditional neuroligin-2
11 knockout in adult medial prefrontal cortex links chronic changes in synaptic inhibition to
12 cognitive impairments. *Mol Psychiatry* 20: 850-859
- 13 Maglioni S, Schiavi A, Melcher M, Brinkmann V, Luo Z, Laromaine A, Raimundo N,
14 Meyer JN, Distelmaier F, Ventura N (2022) Neuroligin-mediated neurodevelopmental
15 defects are induced by mitochondrial dysfunction and prevented by lutein in *C. elegans*.
16 *Nat Commun* 13: 2620
- 17 Marro SG, Chanda S, Yang N, Janas JA, Valperga G, Trotter J, Zhou B, Merrill S, Yousif
18 I, Shelby H et al (2019) Neuroligin-4 Regulates Excitatory Synaptic Transmission in
19 Human Neurons. *Neuron* 103: 617-626 e616
- 20 Nguyen QA, Horn ME, Nicoll RA (2016) Distinct roles for extracellular and intracellular
21 domains in neuroligin function at inhibitory synapses. *Elife* 5
- 22 Nguyen T, Sudhof TC (1997) Binding properties of neuroligin 1 and neurexin 1beta
23 reveal function as heterophilic cell adhesion molecules. *J Biol Chem* 272: 26032-26039
- 24 Pettem KL, Yokomaku D, Takahashi H, Ge Y, Craig AM (2013) Interaction between
25 autism-linked MDGAs and neuroligins suppresses inhibitory synapse development. *J
Cell Biol* 200: 321-336
- 27 Poulopoulos A, Aramuni G, Meyer G, Soykan T, Hoon M, Papadopoulos T, Zhang M,
28 Paarmann I, Fuchs C, Harvey K et al (2009) Neuroligin 2 drives postsynaptic assembly
29 at perisomatic inhibitory synapses through gephyrin and collybistin. *Neuron* 63: 628-642
- 30 Scheiffele P, Fan J, Choih J, Fetter R, Serafini T (2000) Neuroligin expressed in
31 nonneuronal cells triggers presynaptic development in contacting axons. *Cell* 101: 657-
32 669
- 33 Song JY, Ichtchenko K, Sudhof TC, Brose N (1999) Neuroligin 1 is a postsynaptic cell-
34 adhesion molecule of excitatory synapses. *Proc Natl Acad Sci U S A* 96: 1100-1105
- 35 Sudhof TC (2008) Neuroligins and neurexins link synaptic function to cognitive disease.
36 *Nature* 455: 903-911
- 37 Sudhof TC (2017) Synaptic Neurexin Complexes: A Molecular Code for the Logic of
38 Neural Circuits. *Cell* 171: 745-769
- 39 Sun M, Xing G, Yuan L, Gan G, Knight D, With SI, He C, Han J, Zeng X, Fang M et al
40 (2011) Neuroligin 2 is required for synapse development and function at the Drosophila
41 neuromuscular junction. *J Neurosci* 31: 687-699
- 42 Sun Y, Li M, Geng J, Meng S, Tu R, Zhuang Y, Sun M, Rui M, Ou M, Xing G et al (2023)
43 Neuroligin 2 governs synaptic morphology and function through RACK1-cofilin signaling
44 in Drosophila. *Commun Biol* 6: 1056

- 1 Tabuchi K, Blundell J, Etherton MR, Hammer RE, Liu X, Powell CM, Sudhof TC (2007) A
2 neuroligin-3 mutation implicated in autism increases inhibitory synaptic transmission in
3 mice. *Science* 318: 71-76
- 4 Takacs VT, Freund TF, Nyiri G (2013) Neuroligin 2 is expressed in synapses established
5 by cholinergic cells in the mouse brain. *PLoS One* 8: e72450
- 6 Tanaka H, Miyazaki N, Matoba K, Nogi T, Iwasaki K, Takagi J (2012) Higher-order
7 architecture of cell adhesion mediated by polymorphic synaptic adhesion molecules
8 neurexin and neuroligin. *Cell Rep* 2: 101-110
- 9 Treutlein B, Gokce O, Quake SR, Sudhof TC (2014) Cartography of neurexin alternative
10 splicing mapped by single-molecule long-read mRNA sequencing. *Proc Natl Acad Sci U
11 S A* 111: E1291-1299
- 12 Trotter JH, Hao J, Maxeiner S, Tsetsenis T, Liu Z, Zhuang X, Sudhof TC (2019) Synaptic
13 neurexin-1 assembles into dynamically regulated active zone nanoclusters. *J Cell Biol*
14 218: 2677-2698
- 15 Tu H, Pinan-Lucarre B, Ji T, Jospin M, Bessereau JL (2015) C. elegans Punctin Clusters
16 GABA(A) Receptors via Neuroligin Binding and UNC-40/DCC Recruitment. *Neuron* 86:
17 1407-1419
- 18 Tyagarajan SK, Fritschy JM (2014) Gephyrin: a master regulator of neuronal function?
19 *Nat Rev Neurosci* 15: 141-156
- 20 Tyagarajan SK, Ghosh H, Yevenes GE, Nikonenko I, Ebeling C, Schwerdel C, Sidler C,
21 Zeilhofer HU, Gerrits B, Muller D et al (2011) Regulation of GABAergic synapse
22 formation and plasticity by GSK3beta-dependent phosphorylation of gephyrin. *Proc Natl
23 Acad Sci U S A* 108: 379-384
- 24 Uchigashima M, Ohtsuka T, Kobayashi K, Watanabe M (2016) Dopamine synapse is a
25 neuroligin-2-mediated contact between dopaminergic presynaptic and GABAergic
26 postsynaptic structures. *Proc Natl Acad Sci U S A* 113: 4206-4211
- 27 Varoqueaux F, Aramuni G, Rawson RL, Mohrmann R, Missler M, Gottmann K, Zhang W,
28 Sudhof TC, Brose N (2006) Neuroligins determine synapse maturation and function.
29 *Neuron* 51: 741-754
- 30 Varoqueaux F, Jamain S, Brose N (2004) Neuroligin 2 is exclusively localized to
31 inhibitory synapses. *Eur J Cell Biol* 83: 449-456
- 32 Wagner SA, Beli P, Weinert BT, Scholz C, Kelstrup CD, Young C, Nielsen ML, Olsen JV,
33 Brakebusch C, Choudhary C (2012) Proteomic analyses reveal divergent ubiquitylation
34 site patterns in murine tissues. *Mol Cell Proteomics* 11: 1578-1585
- 35 Wang J, Miao Y, Wicklein R, Sun Z, Wang J, Jude KM, Fernandes RA, Merrill SA,
36 Wernig M, Garcia KC et al (2022) RTN4/NoGo-receptor binding to BAI adhesion-
37 GPCRs regulates neuronal development. *Cell* 185: 218
- 38 Wu X, Morishita WK, Riley AM, Hale WD, Sudhof TC, Malenka RC (2019) Neuroligin-1
39 Signaling Controls LTP and NMDA Receptors by Distinct Molecular Pathways. *Neuron*
40 102: 621-635 e623
- 41 Xing G, Gan G, Chen D, Sun M, Yi J, Lv H, Han J, Xie W (2014) Drosophila neuroligin3
42 regulates neuromuscular junction development and synaptic differentiation. *J Biol Chem*
43 289: 31867-31877
- 44 Yamasaki T, Hoyos-Ramirez E, Martenson JS, Morimoto-Tomita M, Tomita S (2017)
45 GARLH Family Proteins Stabilize GABA(A) Receptors at Synapses. *Neuron* 93: 1138-
46 1152 e1136

- 1 Yoshida T, Yamagata A, Imai A, Kim J, Izumi H, Nakashima S, Shiroshima T, Maeda A,
2 Iwasawa-Okamoto S, Azechi K *et al* (2021) Canonical versus non-canonical
3 transsynaptic signaling of neuroligin 3 tunes development of sociality in mice. *Nat*
4 *Commun* 12: 1848
- 5 Zhang B, Chen LY, Liu X, Maxeiner S, Lee SJ, Gokce O, Sudhof TC (2015) Neuroligins
6 Sculpt Cerebellar Purkinje-Cell Circuits by Differential Control of Distinct Classes of
7 Synapses. *Neuron* 87: 781-796
- 8 Zhang B, Gokce O, Hale WD, Brose N, Sudhof TC (2018) Autism-associated neuroligin-
9 4 mutation selectively impairs glycinergic synaptic transmission in mouse brainstem
10 synapses. *J Exp Med* 215: 1543-1553
- 11

1 **FIGURE LEGENDS**

2 **Figure 1. Nlgn1 and Nlgn2 are specifically localized on excitatory and inhibitory**
3 **synapses.**

- 4 A. Schematic overview of experimental timeline and set-up.
- 5 B. Schematic of Nlgn1-WT and Nlgn2-WT constructs.
- 6 C. Representative image from DIV14-16 cultured Nlgn1234 conditional knockout mice
7 neurons, infected with Cre (blue) and either Nlgn1-WT (top) or Nlgn2-WT (bottom). The
8 neurons were labeled with antibodies to Homer1 (red), HA (green), and MAP2 (blue).
9 Scale bar: 20 μ m. The right panels show an enlarged box area (arrowheads indicate HA
10 puncta overlapped with Homer1 puncta). Scale bar: 5 μ m.
- 11 D. Summary graph of the HA-Homer1 overlap percentage in Nlgn1-WT and Nlgn2-WT
12 conditions. (Bar and line graphs indicate mean \pm SEM; numbers of cells/experiments =
13 13/3 and 11/3 for each column, left to right. Statistical significance was assessed by
14 unpaired t test, *** $p<0.0001$).
- 15 E. Representative image of hippocampal neurons from DIV14-16 cultured Nlgn1234
16 conditional knockout mice, infected with Cre (blue) and either Nlgn1-WT (top) or Nlgn2-
17 WT (bottom). The neurons were labeled with antibodies to Gephyrin (red), HA (green),
18 and MAP2 (blue). Scale bar: 20 μ m. The right panels show an enlarged box area
19 (arrowheads indicate HA puncta overlapped with Gephyrin puncta). Scale bar: 5 μ m.
- 20 F. Summary graph of the HA-Gephyrin overlap percentage in Nlgn1-WT and Nlgn2-WT
21 conditions. (Bar and line graphs indicate mean \pm SEM; numbers of cells/experiments =
22 15/3 and 14/3 for each column, left to right. Statistical significance was assessed by
23 unpaired t test, **** $p<0.0001$).

1 **Figure 2. The intracellular sequence of Nlgn2 is necessary for inhibitory synapse
2 function but can be fully replaced with the intracellular sequence of Nlgn1.**

- 3 A. Schematic of Nlgn2-WT, Nlgn2-GPI (Nlgn2 chimeric construct only has extracellular
4 domain), Nlgn2-Nlgn1 (Nlgn2 extracellular domain with Nlgn1 intercellular domain)
5 constructs.
6 B. Representative traces of evoked GABA_A-IPSC recorded from DIV14-16 cultured
7 Nlgn1234 conditional knockout mice neurons in the five conditions (Δ Cre, Cre,
8 Cre+Nlgn2-WT, Cre+Nlgn2-GPI and Cre+Nlgn2-Nlgn1).
9 C. Summary graph of evoked GABA_A-IPSC amplitude in all conditions (Bar and line graphs
10 indicate mean \pm SEM; numbers of cells/experiments = 16/3, 16/3, 16/3, 14/3 and 14/3
11 for each column, left to right). *Nonsignificant p>0.05*; **p<0.01; ***p<0.001;
12 ****p<0.0001, one-way ANOVA with post-hoc Dunnett's Multiple comparisons.
13

1 **Figure 3. The cytoplasmic gephyrin binding motif is required for Nlgn2 function**
2 **whereas tyrosine phosphorylation is not.**

- 3 A. Alignment of Nlgn1 and Nlgn2 gephyrin binding sequence.
- 4 B. Schematic of Nlgn2-Nlgn1Y770A (Nlgn2 extracellular domain with Nlgn1 intercellular
5 domain with a gephyrin binding point mutation), Nlgn2-Nlgn1DelGeph (Nlgn2
6 extracellular domain with Nlgn1 intercellular domain truncation of the entire gephyrin
7 binding sequence) constructs.
- 8 C. Representative traces of evoked GABA-IPSC recorded from DIV14-16 cultured
9 Nlgn1234 conditional knockout mice neurons in the four conditions (Δ Cre, Cre,
10 Cre+Nlgn2-Nlgn1Y770A, Cre+Nlgn2-Nlgn1DelGeph).
- 11 D. Summary graph of evoked GABA-IPSC amplitude in all conditions (Bar and line graphs
12 indicate mean \pm SEM; numbers of cells/experiments = 15/3, 16/3, 15/3, and 15/3 for each
13 column, left to right). *Nonsignificant p>0.05*; *** $p<0.001$, one-way ANOVA with post-hoc
14 Dunnett's Multiple comparisons. Nonsignificant relations are indicated as ns.

15
16

1 **Figure 4. A conserved cytoplasmic 21 residue sequence is necessary for Nlgn2**
2 **function, whereas the PDZ-domain binding sequence is dispensable.**

- 3 A. Alignment of Nlgn1 and Nlgn2 intracellular domain. Colored boxes show the different
4 Nlgn2 intracellular domain truncations.
5 B. Schematic of Nlgn2-mt1, Nlgn2-mt2, Nlgn2-mt3, Nlgn2-mt3, Nlgn2-mt4 and Nlgn2-mt5
6 constructs.
7 C. Representative traces of evoked GABAR-IPSC recorded from DIV14-16 cultured
8 Nlgn1234 conditional knockout mice neurons in the seven conditions (Δ Cre, Cre,
9 Cre+Nlgn2-mt1, Cre+Nlgn2-mt2, Cre+Nlgn2-mt3, Cre+Nlgn2-mt4, Cre+Nlgn2-mt5).
10 D. Summary graph of evoked GABAR-IPSC amplitude in all conditions (Bar and line graphs
11 indicate mean \pm SEM; numbers of cells/experiments = 19/4, 19/4, 19/4, 19/4, 17/4, 13/3,
12 and 13/3 for each column, left to right). *Nonsignificant p>0.05*; ** $p<0.01$; *** $p<0.001$,
13 one-way ANOVA with post-hoc Dunnett's Multiple comparisons. Nonsignificant relations
14 are indicated as ns.
15

1 **Figure 5. Different from the functional promiscuity of the Nlgn1 and Nlgn2**
2 **cytoplasmic sequences, their extracellular sequences encode synapse type-**
3 **specificity that is independent of MDGA binding.**

- 4 A. Schematic of Nlgn1-Nlgn2 (Nlgn1 extracellular domain with Nlgn2 intercellular domain)
5 constructs.
6 B. Representative traces of evoked GABAR-IPSC recorded from DIV14-16 cultured
7 Nlgn1234 conditional knockout mice neurons in the three conditions (Δ Cre, Cre,
8 Cre+Nlgn1-Nlgn2). Note that we rescued Nlgn1-Nlgn2 here from the identical three
9 batches of Figure 2, so the Δ Cre and Cre traces here are the same as in Figure 2.
10 C. Summary graph of evoked GABAR-IPSC amplitude in all conditions (Bar and line graphs
11 indicate mean \pm SEM; numbers of cells/experiments = 16/3, 16/3, and 12/3 for each
12 column, left to right). **** $p<0.0001$, one-way ANOVA with post-hoc Dunnett's Multiple
13 comparisons. Nonsignificant relations are indicated as ns. Note that we rescued Nlgn1-
14 Nlgn2 here from the identical three batches of Figure 2, so the Δ Cre and Cre data here
15 are the same as in Figure 2.
16 D. Schematic of Nlgn2-MDGA1mt (Nlgn2 with MDGA1-binding point mutation) constructs.
17 E. Representative traces of evoked GABAR-IPSC recorded from DIV14-16 cultured
18 Nlgn1234 conditional knockout mice neurons in the three conditions (Δ Cre, Cre,
19 Cre+Nlgn2-MDGA1mt).
20 F. Summary graph of evoked GABAR-IPSC amplitude in all conditions (Bar and line graphs
21 indicate mean \pm SEM; numbers of cells/experiments = 16/3, 15/3, and 18/3 for each
22 column, left to right). **Nonsignificant $p>0.05$** ; ** $p<0.01$, one-way ANOVA with post-hoc
23 Dunnett's Multiple comparisons. Nonsignificant relations are indicated as ns.
24

1 **Figure 6. Nlgn1 extracellular domain provides the specificity of Nlgn1 excitatory**
2 **function.**

- 3 A. Schematic of Nlgn1-WT, Nlgn1-GPI (Nlgn1 chimeric construct only has extracellular
4 domain), Nlgn2-Nlgn1 constructs.
5 B. Representative traces of evoked AMPAR- and NMDAR-EPSCs recorded from DIV14-16
6 cultured Nlgn1^{+/+/-} conditional knockout mice neurons. AMPAR-EPSCs and NMDAR-
7 EPSC recorded at -70 mV and +40 mV, respectively, in the five conditions (Δ Cre, Cre,
8 Cre+Nlgn1-WT, Cre+Nlgn1-GPI, Cre+Nlgn2-Nlgn1).
9 C. Summary graph of evoked AMPAR-EPSC amplitude in all conditions (Bar and line
10 graphs indicate mean \pm SEM; numbers of cells/experiments = 22/4, 17/4, 22/4, 23/4, and
11 16/3 for each column, left to right). *Nonsignificant p>0.05*; *p<0.05, one-way ANOVA with
12 post-hoc Dunnett's Multiple comparisons. Nonsignificant relations are indicated as ns.
13 D. Summary graph of evoked NMDAR-EPSC amplitude in all conditions (Bar and line
14 graphs indicate mean \pm SEM; numbers of cells/experiments = 22/4, 17/4, 22/4, 23/4, and
15 16/3 for each column, left to right). *Nonsignificant p>0.05*; **p<0.01; ****p<0.0001, one-
16 way ANOVA with post-hoc Dunnett's Multiple comparisons. Nonsignificant relations are
17 indicated as ns.
18

1 **Figure 7. Nlgn1 function in excitatory synapses does not require Neurexin-
2 binding, MDGA-binding, or dimerization.**

- 3 A. Schematic of Nlgn1-NRXNmt (Nlgn1 with neurexin-binding point mutation), Nlgn1-dimmt
4 (Nlgn1 dimerization point mutation), Nlgn1-MDGA1mt (Nlgn1 with MDGA1-binding point
5 mutation) constructs.
6 B. Representative traces of evoked AMPAR- and NMDAR-EPSCs recorded from DIV14-16
7 cultured Nlgn1^{-/-} conditional knockout mice neurons. AMPAR-EPSCs and NMDAR-
8 EPSC recorded at -70 mV and +40 mV, respectively, in the five conditions (Δ Cre, Cre,
9 Cre+Nlgn1-NRXNmt, Cre+Nlgn1-dimmt, Cre+Nlgn1-MDGA1mt).
10 C. Summary graph of evoked AMPAR-EPSC amplitude in all conditions (Bar and line
11 graphs indicate mean \pm SEM; numbers of cells/experiments = 17/4, 14/4, 15/4, 18/4, and
12 15/4 for each column, left to right). *Nonsignificant p>0.05*; * $p<0.05$, one-way ANOVA with
13 post-hoc Dunnett's Multiple comparisons. Nonsignificant relations are indicated as ns.
14 D. Summary graph of evoked NMDAR-EPSC amplitude in all conditions (Bar and line
15 graphs indicate mean \pm SEM; numbers of cells/experiments = 17/4, 14/4, 15/4, 18/4, and
16 15/4 for each column, left to right). *Nonsignificant p>0.05*; ** $p<0.01$, one-way ANOVA
17 with post-hoc Dunnett's Multiple comparisons. Nonsignificant relations are indicated as
18 ns.
19

1 **Expanded View Figure LEGENDS**

2 **Figure EV1. Neuroligin protein measurement and co-staining Homer1 with**
3 **Gephyrin in Nlgn1234 cKO cultured hippocampal neurons (related to Fig 1).**

- 4 A. Representative images of western blot for Nlgn1, Nlgn2, and Nlgn3 protein expressions
5 from DIV14-16 cultured Nlgn1234 conditional knockout mice neurons, infected with
6 either ΔCre or Cre. Note that the Nlgn3 antibody detects Nlgn3 (blue arrow) and
7 nonspecific band (red arrow).
- 8 B. Summary graphs of western blot analysis for Nlgn1, Nlgn2, and Nlgn3 protein
9 expressions. (Bar and line graphs indicate mean ± SEM; samples/experiments=3/3. 3
10 technical replicates. Statistical significance was assessed by unpaired t test, *** $p<0.001$;
11 **** $p<0.0001$).
- 12 C. Representative image from DIV14-16 cultured Nlgn1234 conditional knockout mice
13 neurons. The neuron was labeled with antibodies to Homer1 (Green), Gephyrin (red),
14 and MAP2 (blue). Scale bar: 20 μm. The right panels show an enlarged box area
15 (arrowheads indicate Homer1 puncta overlapped with Gephyrin puncta) Scale bar: 5 μm.
- 16 D. Summary graph of Homer1 overlap percentage with Gephyrin and Gephyrin overlap
17 percentage with Homer1 (Bar and line graphs indicate mean ± SEM; numbers of
18 cells/experiment=14/1).

19

1 **Figure EV2. Nlgn2 is specifically localized on inhibitory synapses is determined**
2 **by the extracellular sequence of Nlgn2 and cytoplasmic gephyrin binding motif is**
3 **required whereas tyrosine phosphorylation is not (related to Fig 2, Fig3 and Fig 5).**

- 4 A. Representative image from DIV14-16 cultured Nlgn1234 conditional knockout mice
5 neurons, infected with Cre (blue) and Nlgn2-GPI, Nlgn1-Nlgn2, Nlgn2-Nlgn1, and Nlgn2-
6 MDGA1mt (from top to bottom). The neurons were labeled with antibodies to Gephyrin
7 (red), HA (green), and MAP2 (blue). Scale bar: 20 μ m. The right panels show an
8 enlarged box area (arrowheads indicate HA puncta overlapped with Gephyrin puncta).
9 Scale bar: 5 μ m.
- 10 B. Summary graph of the HA-Gephyrin overlap percentage in Nlgn2-GPI, Nlgn1-Nlgn2,
11 Nlgn2-Nlgn1, and Nlgn2-MDGA1mt conditions.
- 12 C. Summary graph of the surface levels of HA-tagged Nlgn2 forms relative to MAP2 signal.
13 B and C (Bar and line graphs indicate mean \pm SEM; numbers of cells/experiments =
14 10/3, 11/3, 9/3 and 9/3 for each column, left to right. Statistical significance was
15 assessed by one-way ANOVA with post-hoc Dunnett's Multiple comparisons,
16 Nonsignificant $p>0.05$; ** $p<0.01$; **** $p<0.0001$).
- 17 D. Representative image from DIV14-16 cultured Nlgn1234 conditional knockout mice
18 neurons, infected with Cre (blue) and Nlgn2-Nlgn1Y770A and Nlgn2-Nlgn1DelGeph. The
19 neurons were labeled with antibodies to Gephyrin (red), HA (green), and MAP2 (blue).
20 Scale bar: 20 μ m. The right panels show an enlarged box area (arrowheads indicate HA
21 puncta overlapped with Gephyrin puncta). Scale bar: 5 μ m.
- 22 E. Summary graph of the HA-Gephyrin overlap percentage in Nlgn2-Nlgn1Y770A and
23 Nlgn2-Nlgn1DelGeph conditions.
- 24 F. Summary graph of the surface levels of HA-tagged Nlgn2-Nlgn1Y770A and Nlgn2-
25 Nlgn1DelGeph relative to MAP2 signal. E and F (Bar and line graphs indicate mean \pm
26 SEM; numbers of cells/experiments = 19/3 and 12/3 for each column, left to right.
27 Statistical significance was assessed by one-way ANOVA with post-hoc Dunnett's
28 Multiple comparisons, Nonsignificant $p>0.05$; **** $p<0.0001$).

1 **Figure EV3. All Nlgn2 intracellular domain truncation constructs can properly**
2 **traffic to the neuron membrane surface, but Nlgn2-NRXNmt and Nlgn2-dimmt**
3 **constructs traffic to the neuron membrane surface signification decrease**
4 **compared to the Nlgn2-WT construct (related to Fig 4).**

- 5 A. Representative image from DIV14-16 cultured Nlgn1234 conditional knockout mice
6 neurons, infected with Cre (blue) and Nlgn2-mt1, Nlgn2-mt2, Nlgn2-mt3, Nlgn2-mt4 and
7 Nlgn2-mt5 (from left to right). The neurons were labeled with antibodies to HA (green)
8 and MAP2 (blue). Scale bar: 20 μ m.
- 9 B. Representative image from DIV14-16 cultured Nlgn1234 conditional knockout mice
10 neurons, infected with Nlgn2-WT, Nlgn2-NRXNmt, and Nlgn2-dimmt. The neurons were
11 labeled with antibodies to total HA (red) and surface HA (green). Scale bar: 20 μ m.
- 12 C. Summary graph of the surface HA/total HA in Nlgn2-WT, Nlgn2-NRXNmt, and Nlgn2-
13 dimmt conditions (Bar and line graphs indicate mean \pm SEM. numbers of
14 cells/experiments = 10/3, 9/3 and 7/3 for each column, left to right. Statistical
15 significance was assessed by one-way ANOVA with post-hoc Dunnett's Multiple
16 comparisons, **** $p<0.0001$).

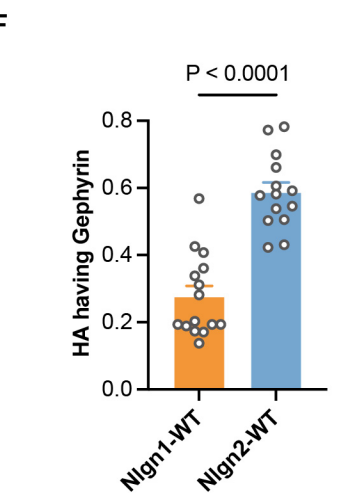
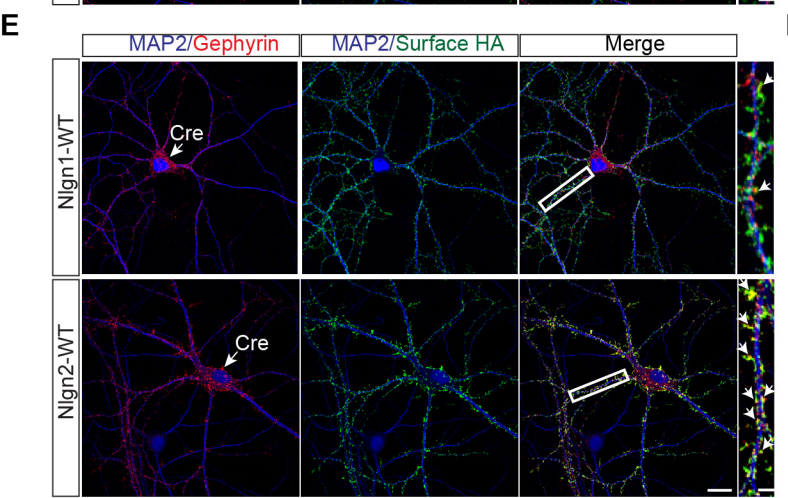
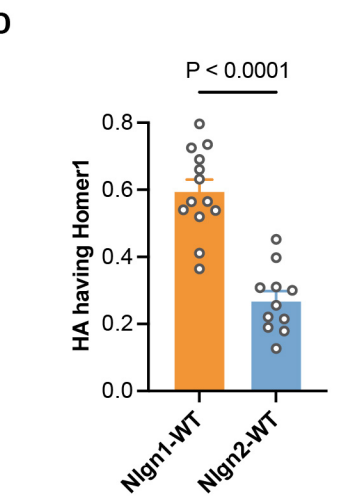
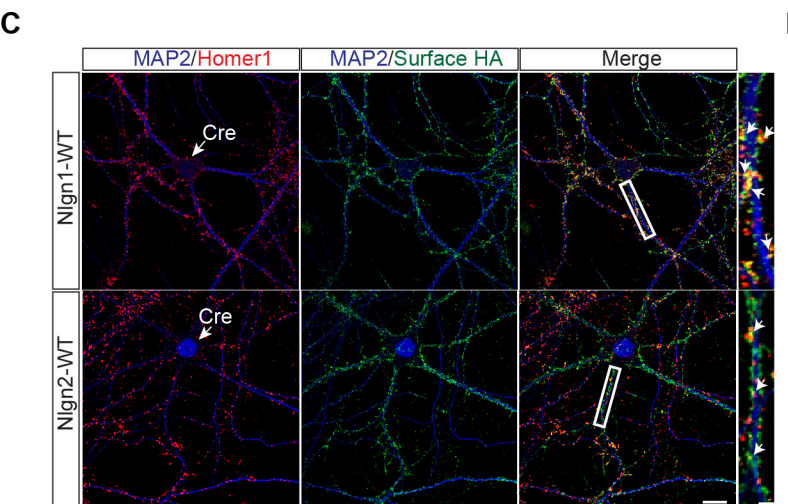
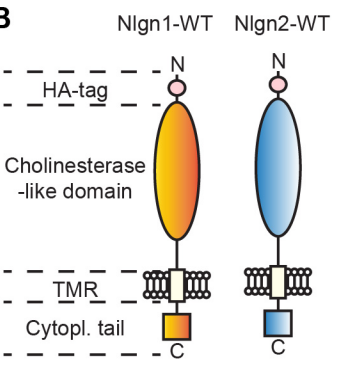
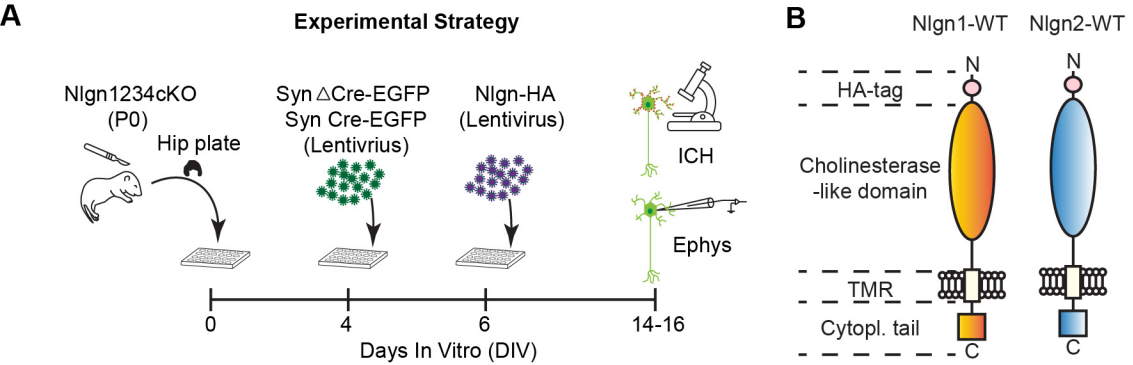
17
18

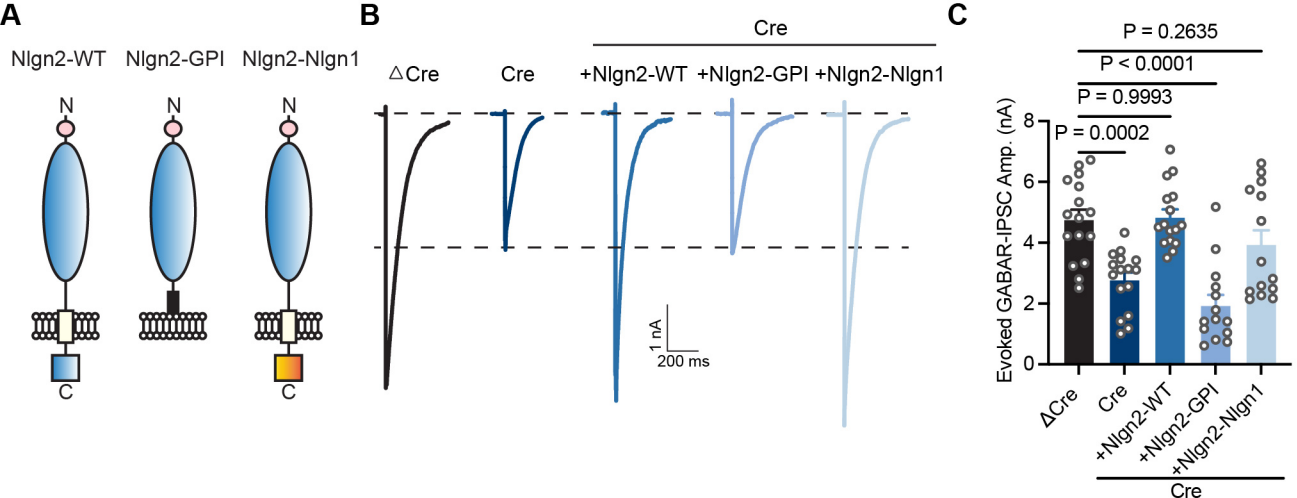
1 **Figure EV4. Nlgn1 is specifically localized on excitatory synapses is determined**
2 **by the extracellular sequence of Nlgn1, and does not require Neurexin-binding,**
3 **MDGA-binding, or dimerization (related to Fig 6 and Fig 7).**

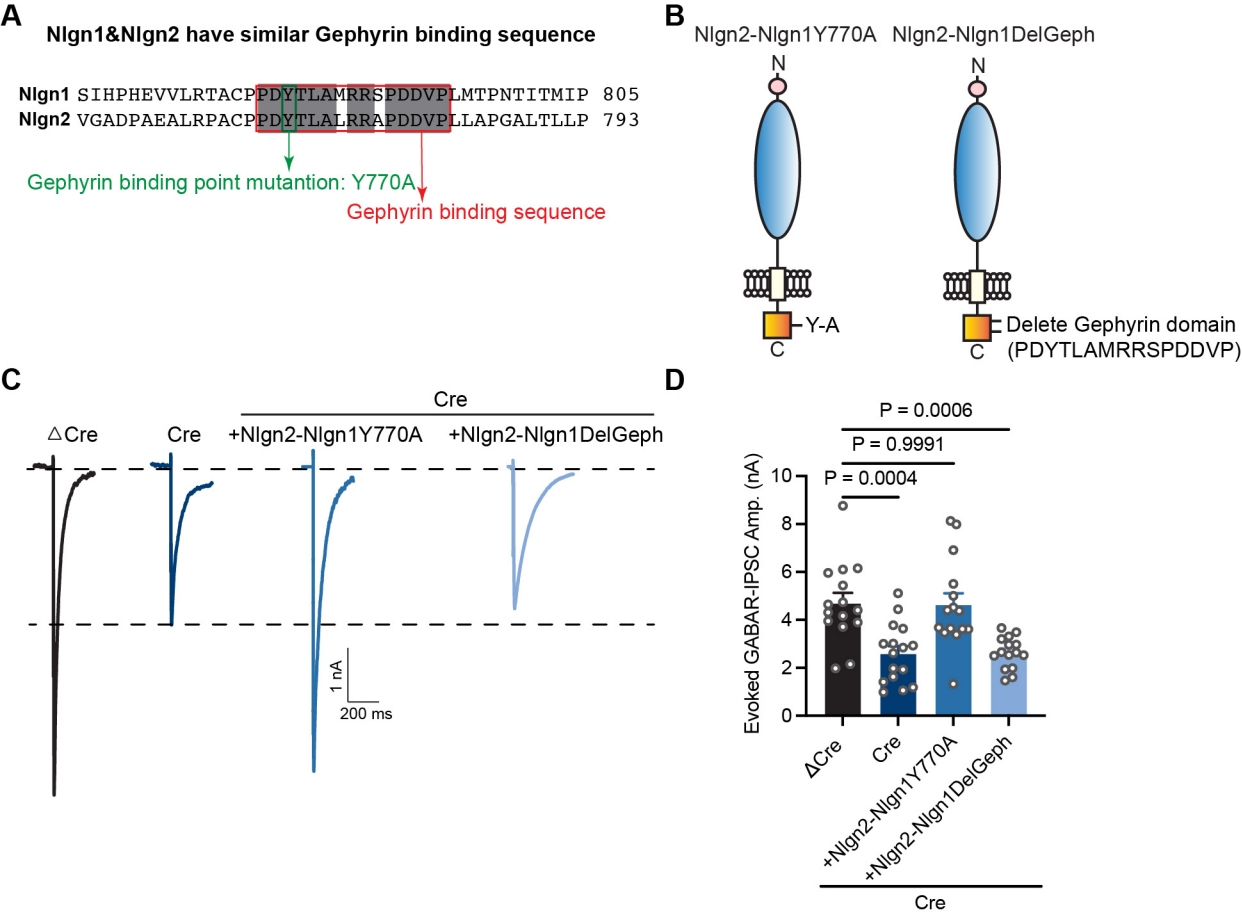
- 4 A. Representative image from DIV14-16 cultured Nlgn1²³⁴ conditional knockout mice
5 neurons, infected with Cre (blue) and Nlgn1-GPI, Nlgn1-Nlgn2, and Nlgn2-Nlgn1. The
6 neurons were labeled with antibodies to Homer1 (red), HA (green), and MAP2 (blue).
7 Scale bar: 20 μ m. The right panels show an enlarged box area (arrowheads indicate HA
8 puncta overlapped with Homer1 puncta). Scale bar: 5 μ m.
- 9 B. Summary graph of the HA-Homer1 overlap percentage in Nlgn1-GPI, Nlgn1-Nlgn2, and
10 Nlgn2-Nlgn1 conditions.
- 11 C. Summary graph of the surface levels of HA-tagged Nlgn1 forms relative to MAP2 signal.
12 B and C (Bar and line graphs indicate mean \pm SEM; numbers of cells/experiments =
13 10/3, 9/3, and 15/3 for each column, left to right. Statistical significance was assessed by
14 one-way ANOVA with post-hoc Dunnett's Multiple comparisons, Nonsignificant $p>0.05$;
15 ** $p<0.01$; *** $p<0.0001$).
- 16 D. Representative image from DIV14-16 cultured Nlgn1²³⁴ conditional knockout mice
17 neurons, infected with Cre (blue) and Nlgn1-NRNXmt, Nlgn1-dimmt, and Nlgn1-
18 MDGA1mt. The neurons were labeled with antibodies to Homer1 (red), HA (green), and
19 MAP2 (blue). Scale bar: 20 μ m. The right panels show an enlarged box area
20 (arrowheads indicate HA puncta overlapped with Homer1 puncta). Scale bar: 5 μ m.
- 21 E. Summary graph of the HA-Homer1 overlap percentage in Nlgn1-NRNXmt, Nlgn1-dimmt,
22 and Nlgn1-MDGA1mt conditions.
- 23 F. Summary graph of the surface levels of HA-tagged Nlgn1 forms relative to MAP2 signal.
24 E and F (Bar and line graphs indicate mean \pm SEM; numbers of cells/experiments =
25 14/3, 9/3, and 9/3 for each column, left to right. Statistical significance was assessed by
26 one-way ANOVA with post-hoc Dunnett's Multiple comparisons, Nonsignificant $p>0.05$).

1 **Figure EV5. Nlgn1-Nlgn2 is sufficient for the glutamatergic synaptic transmission**
2 **function of Nlgn1, but Nlgn2-WT doesn't (related to Fig 6).**

- 3 A. Summary graph of evoked AMPAR-EPSC amplitude in all conditions (Bar and line
4 graphs indicate mean \pm SEM; numbers of cells/experiments = 22/4, 17/4, 22/4, 7/2, and
5 11/3 for each column, left to right). Nonsignificant $p>0.05$; * $p<0.05$, one-way ANOVA with
6 post-hoc Dunnett's Multiple comparisons. Nonsignificant relations are indicated as ns.
7 Note that we rescued Nlgn1-Nlgn2 and Nlgn2-WT here from the same batches of Figure
8 6, so the Δ Cre and Cre data here are the same as in Figure 6.
- 9 B. Summary graph of evoked NMDAR-EPSC amplitude in all conditions (Bar and line
10 graphs indicate mean \pm SEM; numbers of cells/experiments = 22/4, 17/4, 22/4, 7/2, and
11 11/3 for each column, left to right). Nonsignificant $p>0.05$; *** $p<0.001$; **** $p<0.0001$, one-
12 way ANOVA with post-hoc Dunnett's Multiple comparisons. Nonsignificant relations are
13 indicated as ns. Note that we rescued Nlgn1-Nlgn2 and Nlgn2-WT here from the same
14 batches of Figure 6, so the Δ Cre and Cre data here are the same as in Figure 6.
- 15

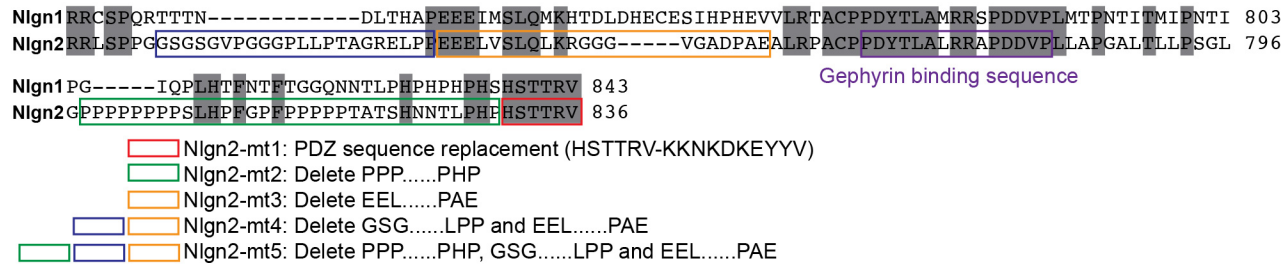
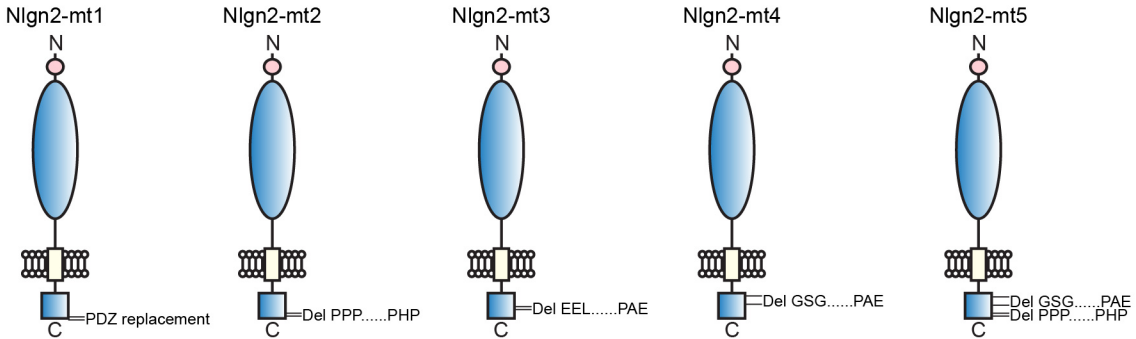
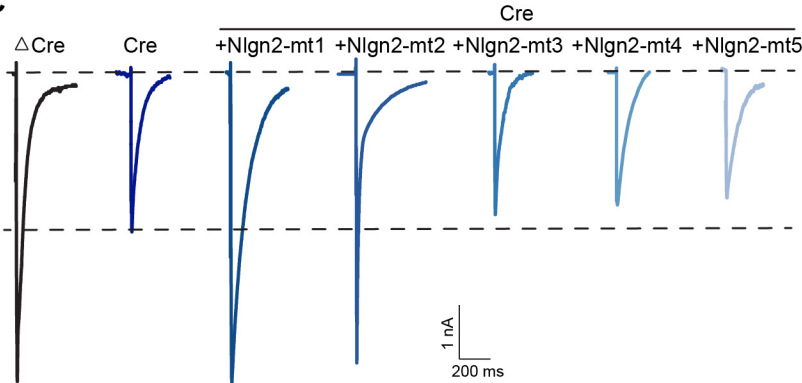
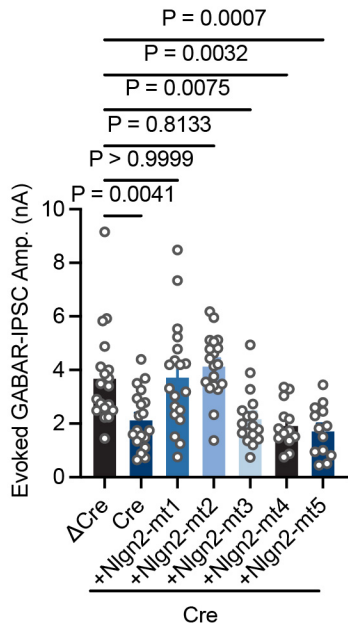


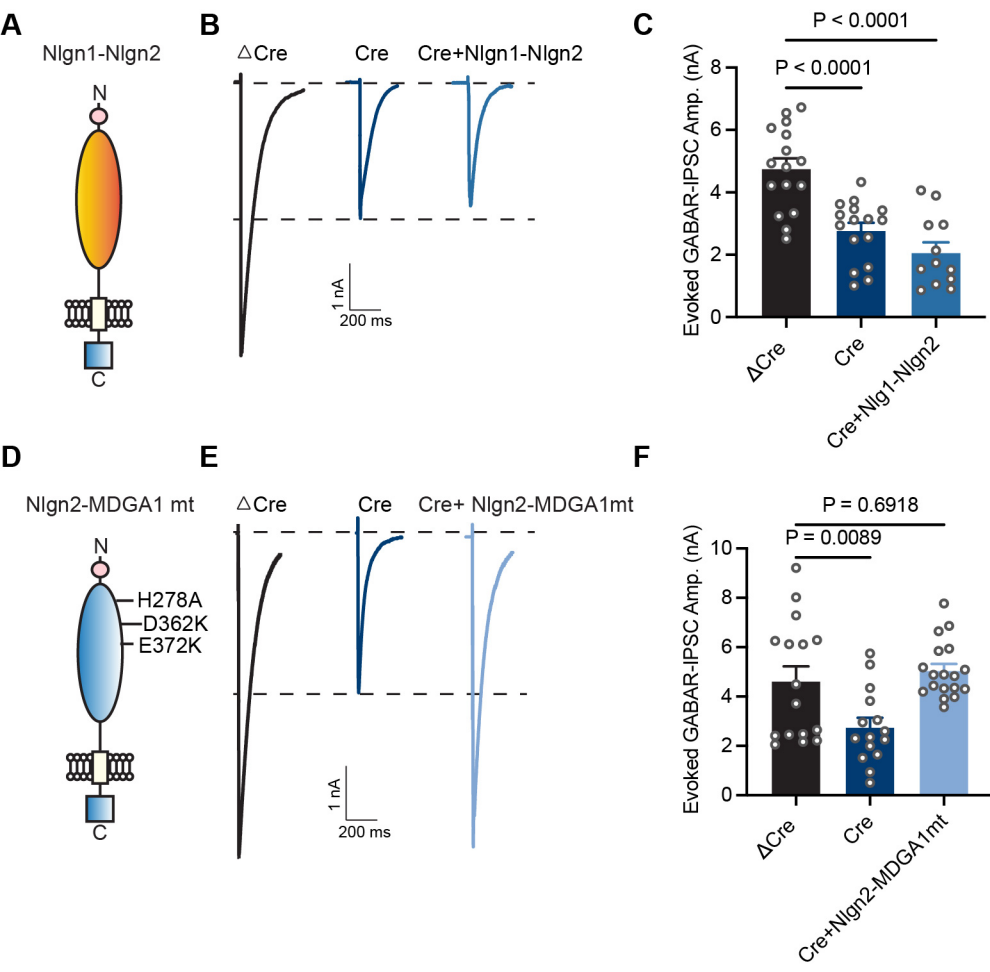


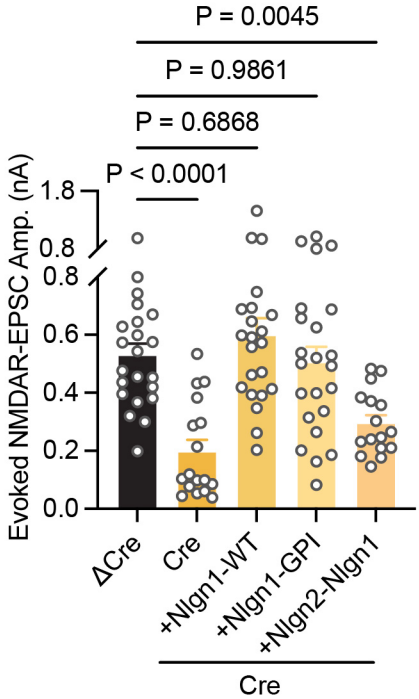
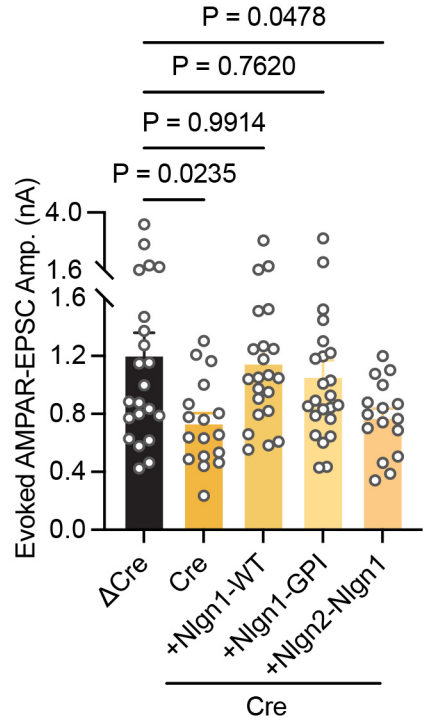
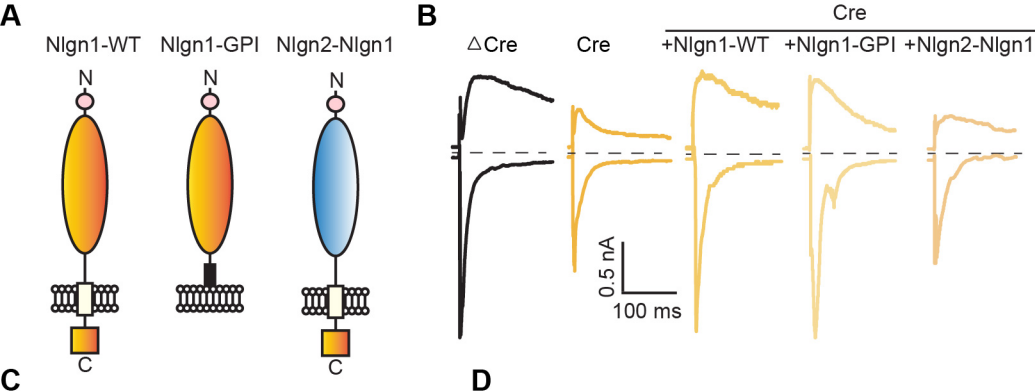


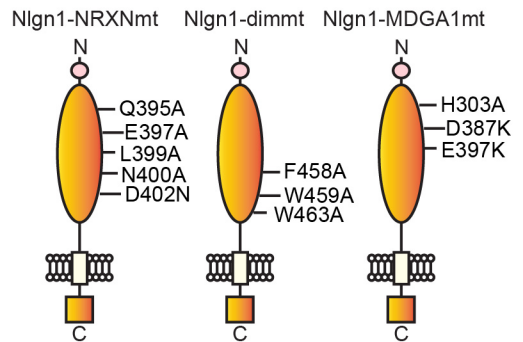
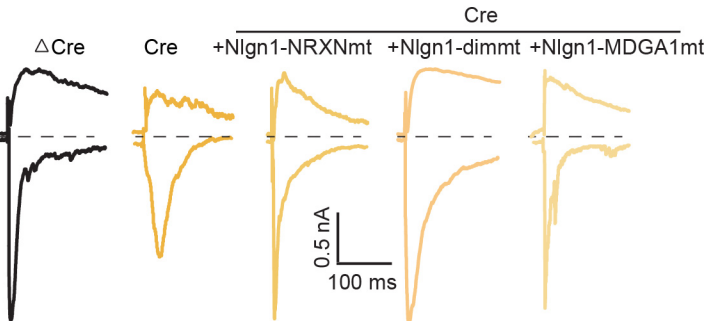
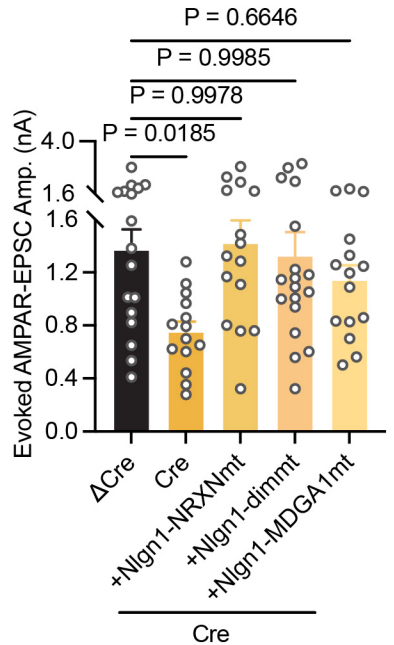
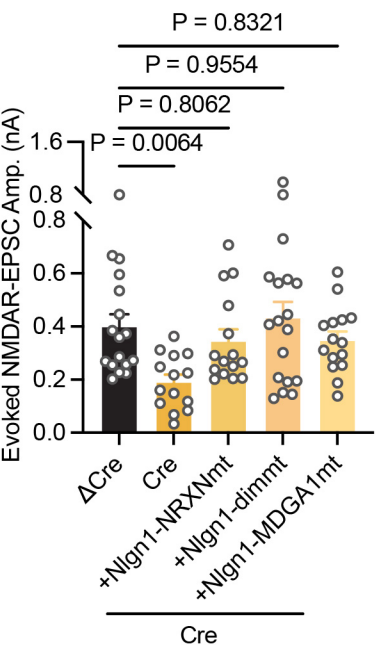
A

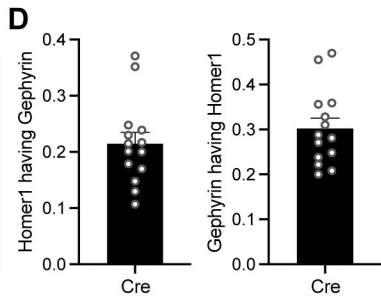
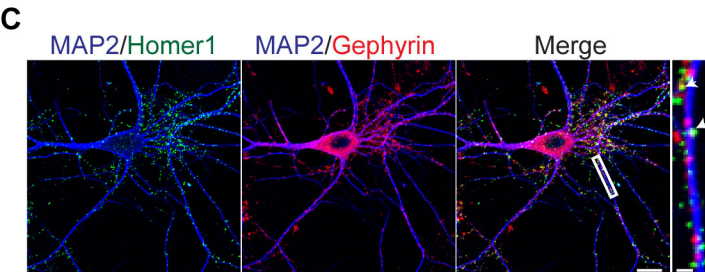
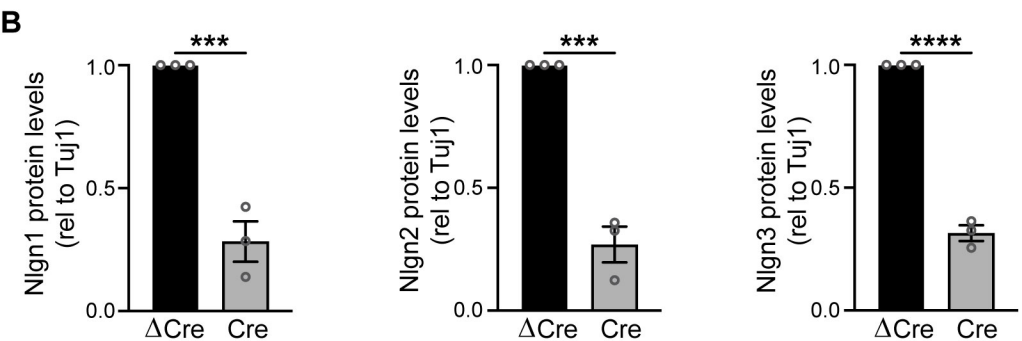
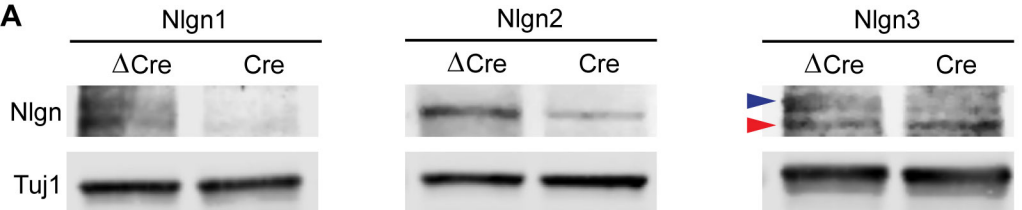
Alignment of Nlgn1&2 intracellular sequence

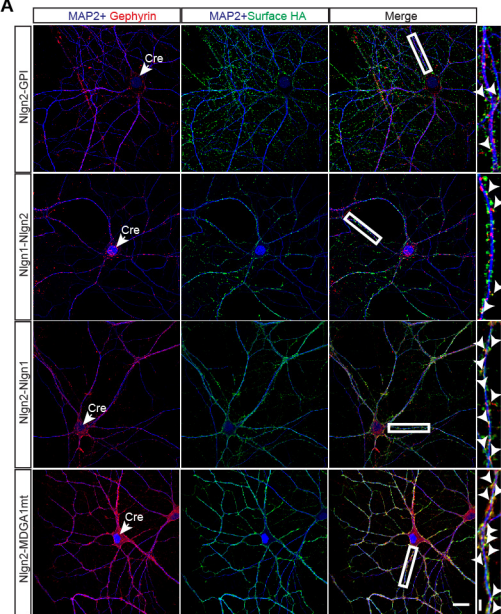
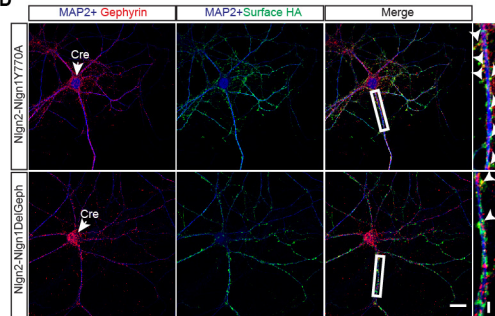
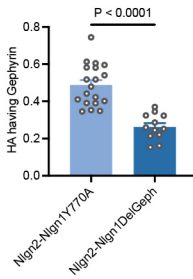
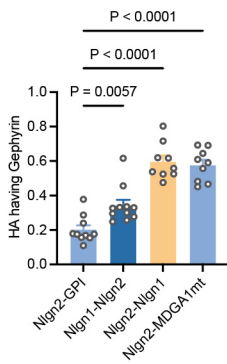
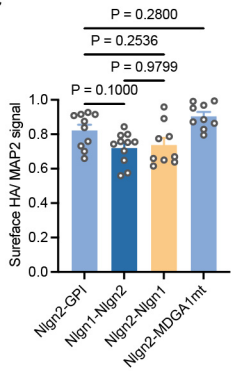
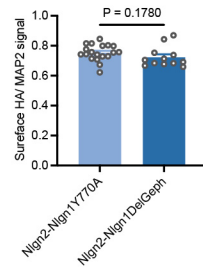
**B****C****D**

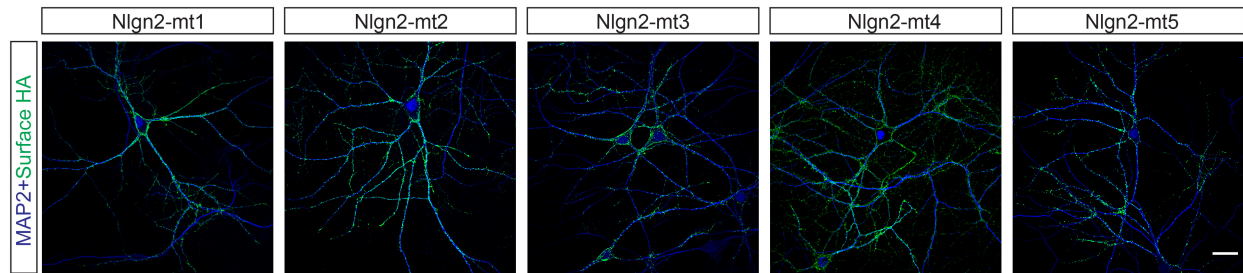




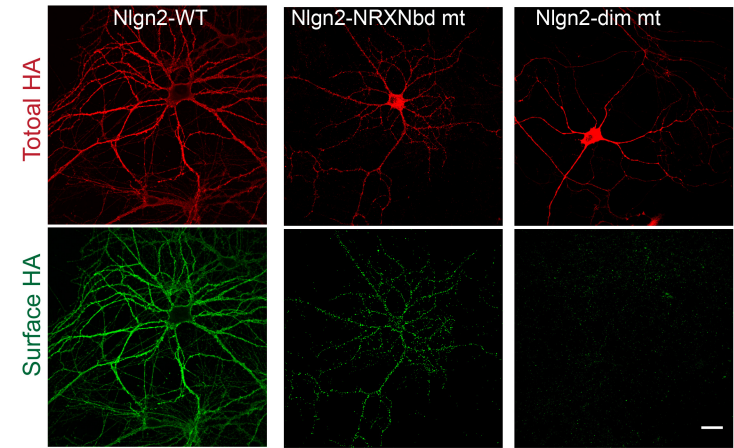
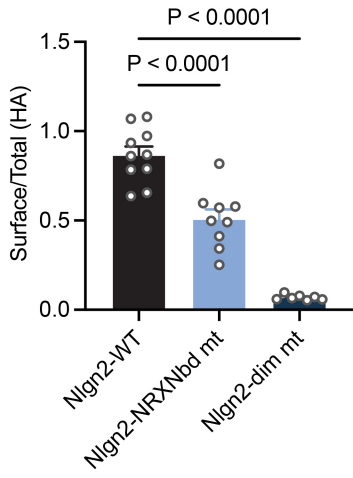
A**B****C****D**

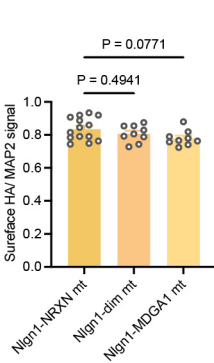
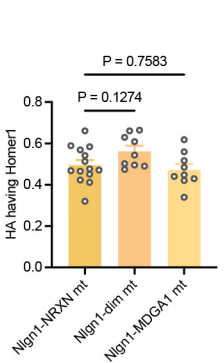
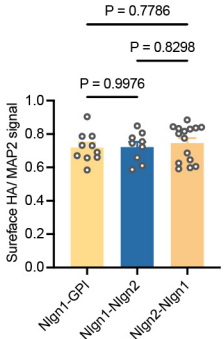
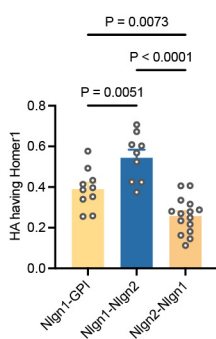
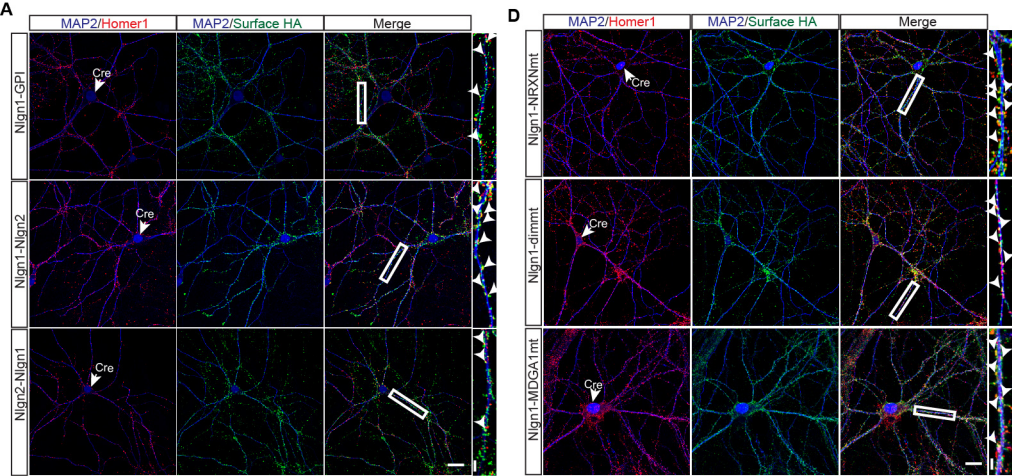


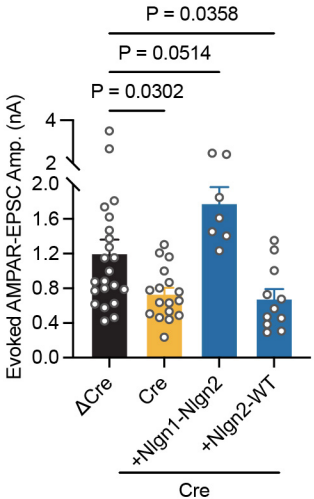
A**D****E****B****C****F**

A**B**

*Surface Expression-Nlgn2
(With Lenti-Cre)*

**C**



A**B**